1950

Deflection of a flexible pipe culvert when stressed beyond the elastic limit

Abu Sharf Misih-ur Rahman
Iowa State College

NOTE TO USERS

DEFLECTION OF A FLEXIBLE PIPE CULVERT WHEN STRESSED BEYOND THE ELASTIC LIMIT

by

Abu Sharf Masih-ur Rahman

A Dissertation Submitted to the
Graduate Faculty in Partial Fulfillment of
The Requirements for the Degree of
DOCTOR OF PHILOSOPHY

Major Subject: Highway Engineering

Approved:

Signature was redacted for privacy.

In Charge of Major Work

Signature was redacted for privacy.

Head of Major Department

Signature was redacted for privacy.

Dean of Graduate College

Iowa State College
1950

To:

THE TWO MOST OUTSTANDING CHARACTERS
I HAVE EVER KNOWN IN MY LIFE....

My late father,

MATIUR RAHMAN

My ex-professor,

ABUL MOHSIN AHMED

TABLE OF CONTENTS

NOTATIONS

A $\frac{2S_0}{Ed}$.

a Radius of the deflected ring measured perpendicularly to the line of action of the load; semi-major axis of an elliptic ring.

b Radius of the deflected ring measured along the line of action of the load; semi-minor axis of an elliptic ring; width of the ring.

2d Thickness of the ring section.

$2d_0$ Thickness of the elastic portion of the ring section when the ring section has partially gone into plastic range of stress.

E Modulus of elasticity of ring material for tension and compression; elliptic integral of the second kind.

e Circumferential strain in the ring section due to the concentrated load; modulus of passive pressure of the sidefill.

F Elliptic integral of the first kind.

H Horizontal thrust at any section of the loaded ring.

h Maximum horizontal unit pressure on the flexible pipe due to the sidefill.

I Moment of inertia of the ring section

k Constants from Burke's graphs.

M Bending moment.

M_B Bending moment at the ring section directly under the concentrated load.

M_A Bending moment at the section 90^0 from the section of the ring directly under the concentrated load.

M_0 Maximum resisting moment the ring section can develop without going into the plastic range of stress.

N $\frac{R_2}{R_1}$

P Concentrated load.

P_0 Maximum concentrated load the ring can be subjected to without putting it into plastic range of stress.

Q $-Ar^2R_1^{-1/2}$

R_1 $1 + \frac{Pr}{M_0}(1-\sin\alpha)$

R_2 $\frac{2Pr}{M_0}$

r Initial mean radius of the ring.

S unit stress.

S_0 Proportional limit.

t Thickness of corrugated pipe

u $\frac{d_0}{d}$

w Uniformly distributed load.

x Rectangular coordinate.

y Radial deflection of the loaded ring at any section, rectangular coordinate.

y_e Radial deflection of the loaded ring in the elastic portion.

y_p Radial deflection of the loaded ring in the partially plastic portion.

$y_{\theta=\frac{\pi}{2}}, \Delta_y$ Radial deflection of the loaded ring directly under the load.

$y_{\theta=0}, \Delta_x$ Radial deflection of the loaded ring 90° from the point of application of the load.

ds Differential length of ring.

α Angle denoting the plastic boundary.

ϵ Unit normal strain.

ϵ_0 Unit strain at the proportional limit.

ϵ_m Unit strain in the extreme inner and outer fiber of the loaded ring.

θ, ϕ, ψ Angles.

π 3.142.

$\frac{1}{\rho}$ Curvature of the loaded ring at any section.

I. INTRODUCTION

A. Usefulness of Flexible Pipes in Construction

Flexible pipe has been used in different types of construction for the last half-century or more. One of the most important uses of flexible pipe is in the construction of culverts and other underground conduits. When used as an underground conduit it is usually corrugated for extra strength. Use of corrugated-metal pipe as cross-drainage structures in highways, railways and airport construction has increased greatly in the last fifty years, particularly due to the fact that it is much lighter in weight than similar concrete or other rigid pipes. Also it is advantageous because of ease of transportation and installation.

In the early days of flexible pipe culvert, its use was restricted mainly to the smaller waterways and drainage areas and its size very seldom exceeded 36 in. in diameter. In those days the height of fill over the pipe culvert usually was not adequate. In some cases it was even too low to protect the culvert from the live traffic load. With the increase of experience of the engineers and its use, the pipe culverts were made in larger diameters and the heights of the fills were increased sufficiently so that practically

they were no longer subjected to the live load due to the traffic. Deep under the earth fill the pipe culvert had to carry only the dead load due to the mass of earth above and adjacent to it.

B. Need for Investigation

At the early stage of usage of flexible pipe culvert no successful attempt was made to develop a rational method for designing this structure according to the principles of mechanics. Engineers rather placed their reliance almost wholly on the service experience and intuition.

In 1941 M. G. Spangler (17) at Iowa State College authored a bulletin published by the Iowa Engineering Experiment Station. In the bulletin Spangler made an extensive investigation on the structural design of flexible pipe culverts under different loading conditions, the culverts being stressed within the elastic limit. Spangler established a rational formula for the horizontal deflection of a flexible pipe culvert under field load condition according to his fill-load hypothesis (17-p.26). As the criterion of failure of an underground flexible conduit is excessive deflection, Spangler's equation gave engineers a long sought for rational method to design the underground flexible pipe culverts stressed within the elastic limit.

Subsequently with the idea of limit design (19) coming into engineering practice more and more it was felt that underground conduit which at the present day carry only a certain amount of dead load due to the earth fill, might successfully and economically be loaded stressing beyond its elastic limit. This idea demanded both theoretical and experimental investigation of the deflection behavior of a flexible pipe culvert when stressed beyond the elastic limit. As a matter of fact, at present there are some flexible pipe culverts in successful use, which, in all probability are stressed beyond the elastic limit. The purpose of this investigation is to establish a procedure by which it will be possible to predict the deflection characteristics of a flexible pipe culvert when stressed beyond the elastic limit.

C. Review of Literature

The study of the mechanics of the plastic state of matter, the theory of plasticity, is still in a formative stage even though it was formulated by B. de St. Venant (1797-1886) more than 75 years ago.

In 1864 St. Venant presented what is known today as the complete mathematical basis for the theory of elasticity, which included the principle of plane section before bending remaining plane after bending. He analysed the cases explicitly in which the principle holds. St. Venant was one of the first to

attempt to solve the problem of plastic bending.

In 1908 Eugene von Meyer (11), Charlottenburg, published the results of an experimental investigation with simply supported beams loaded at the center with a concentrated load where the material did not obey the Hooke's Law.

In 1932 Hans Bleich (2) developed a theory of plastic bending for beams. This theory became the basis for the limit design method as conceived by Van Den Broek in 1939 (19). Later on Van Den Broek wrote a book on theory of limit design (20) in which he shows how it is possible to design a structure which may carry loads beyond its elastic limit at certain points and still be safe from the engineering point of view. Bleich is credited with the idea of the idealized stress-strain diagram. He also developed an expression for the ratio between the resisting moment a section develops when acting partly plastically and the maximum value it develops when acting purely elastically.

In 1938 E. O. Scott (15) at the University of Michigan investigated deformation of beams involving ductile behavior. In 1940 George Winter at Cornell University, investigated plastic bending of beams (21). In 1941 W. T. Daniels (4) at Iowa State College investigated deflection of rigid frames stressed beyond the yield point.

A. Nadai (12) has investigated the problem of plastic bending of beams in which strain hardening was taken into account. He also developed an equation for the internal resisting

moment of the beam, an equation for plastic boundary curve, and showed how the neutral axis position may be determined for loads which cause the beam to be plastically bent.

In 1943 Giulio Pizzetti (13) published a paper concerning elasto-plastic flexure of a bar with pronounced initial curvature. In 1945 C. B. Biezeno and J. J. Koch (1) made an investigation on the generalized buckling problem of the circular ring. In 1946 L. M. Kachanov (10) made a study on the stress-strain relations in the theory of plasticity. In the same year A. Gleyzal (5) investigated general stress-strain laws of elasticity and plasticity. In 1947 A. A. Ilyushin (7) published a report on the theory of plasticity in case of simple loading of plastic bodies with strain hardening. Ilyushin (6) published another paper on the continuation of the same topic in 1949. In 1948 William Prager (14) wrote a paper on the stress-strain laws of the mathematical theory of plasticity. In the paper Prager has made a survey of the recent progress of the subject.

The theories of the deformation of materials stressed beyond the elastic limit may be divided into two groups. In the first group it is assumed that there exists a definite relation between 'stress' and 'velocity strain', which is called the 'theory of plastic flow'. This theory has been developed by St. Venant, Levy and Von Mises and in recent years by G. I. Taylor (18) and his co-workers. In the second

group it is assumed that there exists a definite relation between stress and strain, which is called the 'theory of plastic deformation'. This theory has been developed by H. Hencky and A. Nadai (12). A. A. Ilyushin (8) has discussed in detail the relationship of these two theories and established a general condition for the agreement of their predictions.

The essential difference between the two theories is the following. According to the theory of plastic flow, the instantaneous stress is determined by the instantaneous velocity strain. According to the theory of plastic deformation the instantaneous stress is determined by the instantaneous strain and, hence, by the entire history of velocity strain rather than by the instantaneous velocity strain. In view of such different basic assumptions, it may appear that experimental results should confirm one and contradict the other theory. However, there are no experiments described in any literature which contradict the theory of plastic flow under the conditions at which the theory of plastic deformation is well supported.

As a rule, analyses based on the theory of plastic flow are rather complicated because the deformation process must be treated as an infinite sequence of infinitesimal changes of state. In certain types of problems, for instance, for uniaxial stress, and hence for the analysis of plastic stresses in trusses and beams, the distinction between the theory of

plastic flow and that of plastic deformation becomes insignificant. In view of the relative mathematical simplicity of the theory of plastic deformation and the fact that experimental works published so far are in good agreement with both the theories, this investigation has been based on the theory of plastic deformation.

D. The Problem

Very little investigation has been done so far with the deflection of a flexible circular ring under different loading conditions when plastic action exists in the ring. According to the author's knowledge no literature is available which deals with the prediction of deflection of a flexible circular ring when it is loaded beyond the elastic limit.

The aim of this investigation is to establish a prediction equation for the deflection of a circular ring under two equal and opposite concentrated loads, when the ring is stressed beyond the elastic limit. It may be appreciated that the problem of the deflection of a flexible circular ring of rectangular cross section and that of a flexible circular pipe under same loading system is essentially the same if the effect of axial stress on the pipe due to the load, which is very small, be neglected. This investigation is primarily a theoretical analysis, where the flexible ring is considered to have a rectangular cross section, and the concentrated

load is a line load rather than a point load. The line load consideration makes the results of the investigation readily transferable to the case of flexible pipes. As a test of the validity of the investigation the theoretical solution obtained from the prediction equation has been compared with the results of tests on corrugated flexible pipes. As the corrugation on a pipe increases its moment of inertia, in each case the theoretical solution has been obtained for a circular pipe of equivalent moment of inertia.

II. THEORETICAL SOLUTION OF THE PROBLEM

A. Fundamental Theory

a. Idealized stress-strain diagram. For metals which have definite yield points, such as soft annealed wrought iron, mild steel, etc., the stress-strain curve may be represented, for the purpose of calculation as in Fig. 1. Up to the point A the stress and strain of the test specimen increases proportionately. At the point A

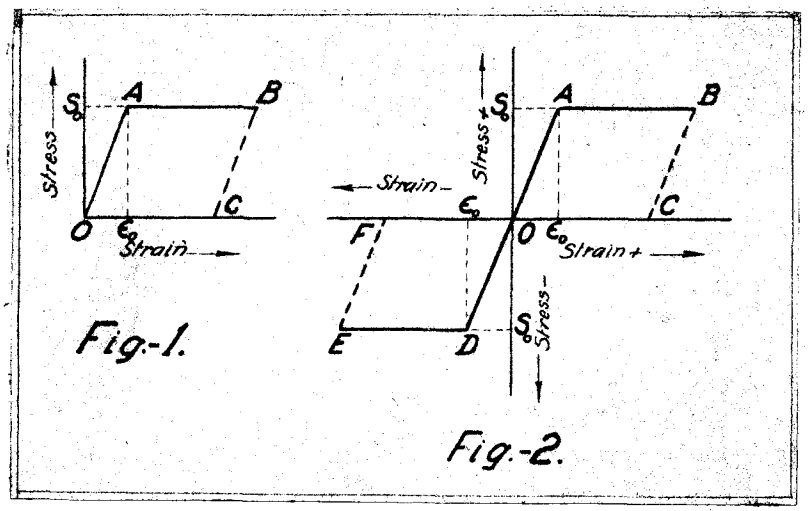

the material of the test specimen yields and the strain in the specimen increases without any appreciable increase of stress in the material. Thus the stress at the point A represents both 'elastic limit' and 'yield point' of the material of the test specimen. If the specimen is unloaded when the curve reaches point B, the line BC will represent the unloading

curve. The amount of permanent strain left in the specimen per unit length will be represented by OC. Mathematically, the loading portion of the stress-strain curve (OAB) can be represented as follows:

for $\epsilon \leq \epsilon_0$, $S = E\epsilon$ where E = modulus of elasticity of the material

for $\epsilon > \epsilon_0$, $S = S_0 = \text{Const.}$, S_0 = yield stress of the material.

Such a stress-strain curve is termed as 'idealized', for experimenters have found that near the point A the curve is not exactly straight and parallel to the strain axis. Some investigators, however, claim that the curve is very close as drawn in Fig. 1, and believe that the cause of variations as observed from the idealized curve may be due to the test specimen or the machine operation.

If it be assumed that the yield points for tension and compression are the same and the moduli of elasticity for tension and compression are also the same, which are very closely true for metals like wrought iron, steel, etc., the stress-strain diagram may be represented by the following conditions (Fig. 2):

for $\epsilon < -\epsilon_0$, $S = -S_0 = \text{Const.}$

for $-\epsilon_0 \leq \epsilon \leq \epsilon_0$, $S = E\epsilon$,

for $\epsilon > \epsilon_0$, $S = S_0 = \text{Const.}$

If a mild steel bar of rectangular section is bent plastically, two kinds of stress regions are developed inside the bar. At the top and bottom of the bar section are stresses, which are equal to the yield point stress of the material. In the center of the section the stresses are elastic and are linearly proportional to the strains. A stress distribution diagram at the section is shown by Fig. 3. It may be noted that the strains are assumed to be constant in a plane parallel to the neutral surface of the section.

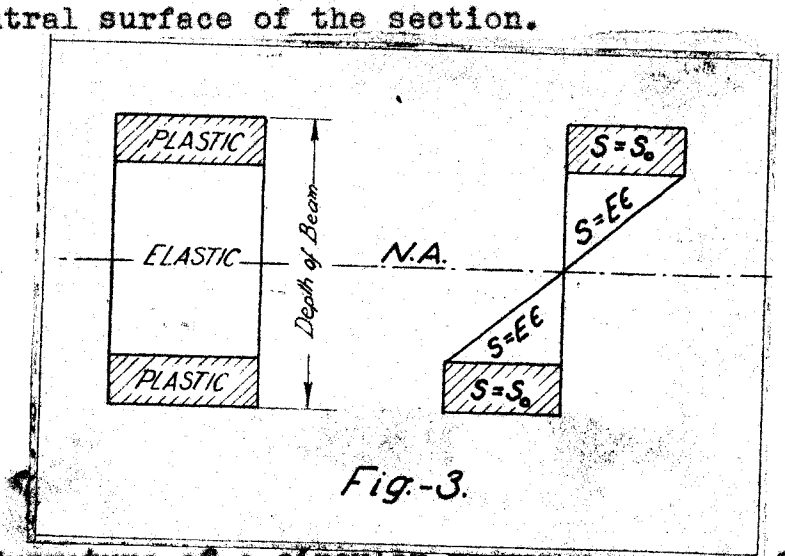

Fig.-3.

b. Curvature of a circular ring under load, expressed approximately as a function of its initial radius and radial deflection. By calculus the equation of curvature in polar coordinates is given as

$$\frac{1}{\rho} = \frac{\left[r_1^2 + 2(r_1')^2 - r_1 r_1''\right]}{\left[r_1^2 + (r_1')^2\right]^{\frac{1}{2}}} \qquad (1)$$

In Eq. 1, ρ = radius of curvature; r_1 = variable radius of the ring; $r_1' = \frac{dr_1}{d\theta}$; $r_1'' = \frac{d^2r_1}{d\theta^2}$. Let us represent r_1 by r-y, where r is the original radius of the ring and y is the variation of r in radial direction. It may be noted here that y ordinarily will be a small quantity. Since r_1' is a small quantity $(r_1')^2$ will be neglected in this analysis.

Eq. 1 then becomes

$$\frac{1}{\rho} = \frac{r_1^2 - r_1 r''}{(r_1^2)^{\frac{3}{2}}} .$$

Since

$$r_1 = r-y, \quad r_1^2 = r^2 - 2ry + y^2$$

$$r_1' = -y', \quad y' = \frac{dy}{d\theta}$$

$$r_1'' = -y'', \quad y'' = \frac{d^2y}{d\theta^2} .$$

Then

$$\frac{1}{\rho} = \frac{r^2 - 2ry + y^2 - (r-y)(-y'')}{(r^2 - 2ry + y^2)^{\frac{3}{2}}} . \qquad (1a)$$

If we neglect small quantities like y^2 and yy'', Eq. 1a becomes,

$$\frac{1}{\rho} = \frac{r^2 - 2ry + ry''}{(r^2 - 2ry)^{\frac{3}{2}}}$$

$$= \frac{r^2 - 2ry + ry''}{r^3(1 - \frac{2y}{r})^{\frac{3}{2}}}$$

$$= \frac{1}{r^3}(r^2 - 2ry + ry'')(1 - \frac{2y}{r})^{-\frac{3}{2}}$$

$$= \frac{1}{r^3}(r^2 - 2ry + ry'')(1 + \frac{3y}{r}) ,$$

or

$$\frac{1}{\rho} = \frac{1}{r^3}(r^2 - 2ry + ry'' + 3ry - 6y^2 + 3yy'').$$

Since y^2 and yy'' may be neglected, then Eq. 1a becomes

$$\frac{1}{\rho} = \frac{1}{r^3}(r^2 + ry + ry''),$$

or

$$\frac{1}{\rho} = \frac{1}{r} + \frac{y}{r^2} + \frac{y''}{r^2} . \qquad (2)$$

c. Geometrical relationship between the change in curvature and circumferential strain in the ring due to the load.

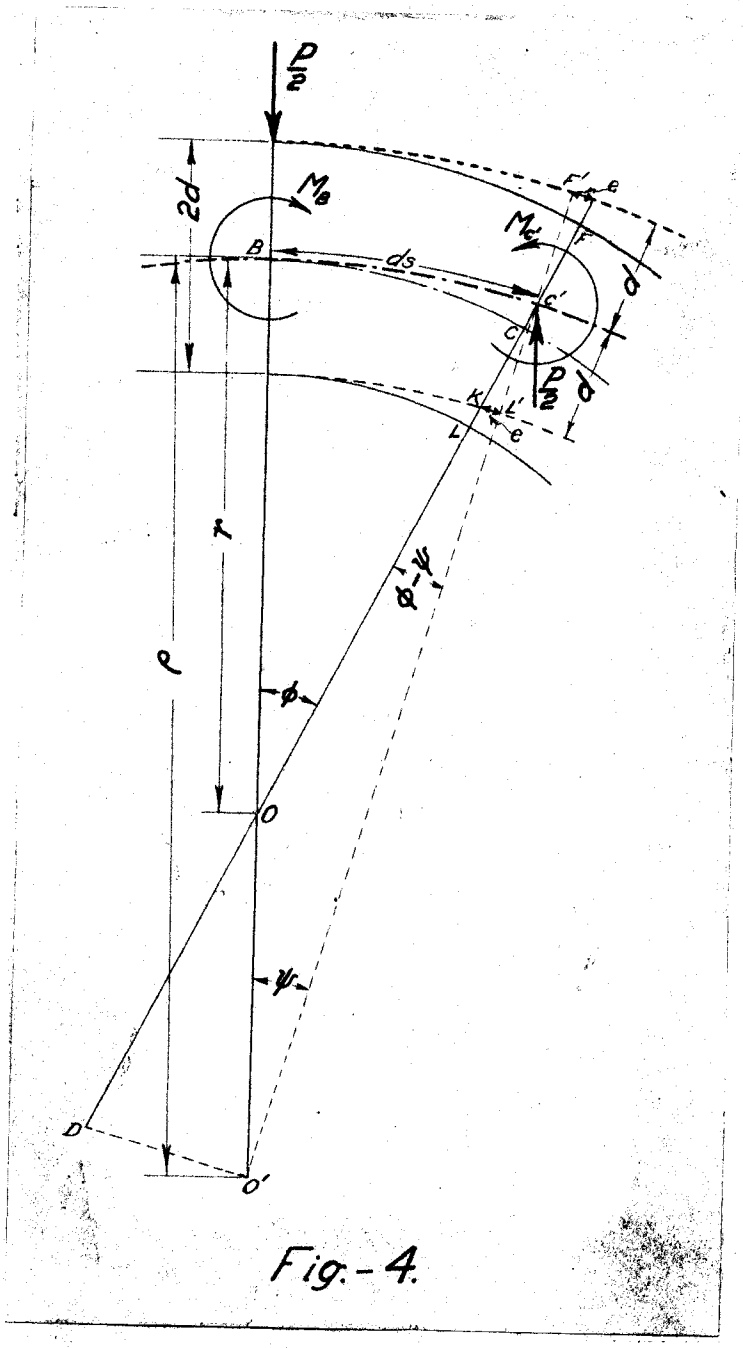

Fig.-4.

Let Fig. 4 represent an element BC of the ring of differential length ds, whose initial radius is r. After the application of the load the radius of the ring changes to ρ. If we consider that a plane section before bending remains plane after bending, the section LCF assumes the new position L'C'F'. The elongation of any fiber at any distance from the neutral surface may be obtained by drawing a line through C' parallel to CO. In Fig. 4 KL' represents e, the total extension of the innermost fiber of the ring. Since triangles C'L'K and C'O'D are similar,

$$\frac{L'K}{L'C'} = \frac{O'D}{O'C'} . \qquad (a)$$

In Eq. (a), L'K = e; L'C' = d; O'D = $\rho(\phi-\psi)$; O'C' = ρ . Substituting these values in Eq. (a), we get,

$$\frac{e}{d} = \frac{\rho(\phi-\psi)}{\rho} = (\phi-\psi). \qquad (b)$$

Since e = ds × ϵ_m, where ϵ_m is the strain in the extreme inner fiber of the ring, $\phi = \frac{ds}{r}$, and $\psi = \frac{ds}{\rho}$. Eq. (b) can be written

$$\frac{ds \times \epsilon_m}{d} = ds\left(\frac{1}{r} - \frac{1}{\rho}\right),$$

or

$$\frac{\epsilon_m}{d} = \frac{1}{r} - \frac{1}{\rho} . \qquad (3)$$

d. Equation for internal moment of a rectangular section when it is partially in plastic range of stress. Using the idealized stress-strain diagram, the cross-section of the ring, stress distribution in the section and the stress-strain relationship may be represented as in Figs. 5a, 5b and 5c.

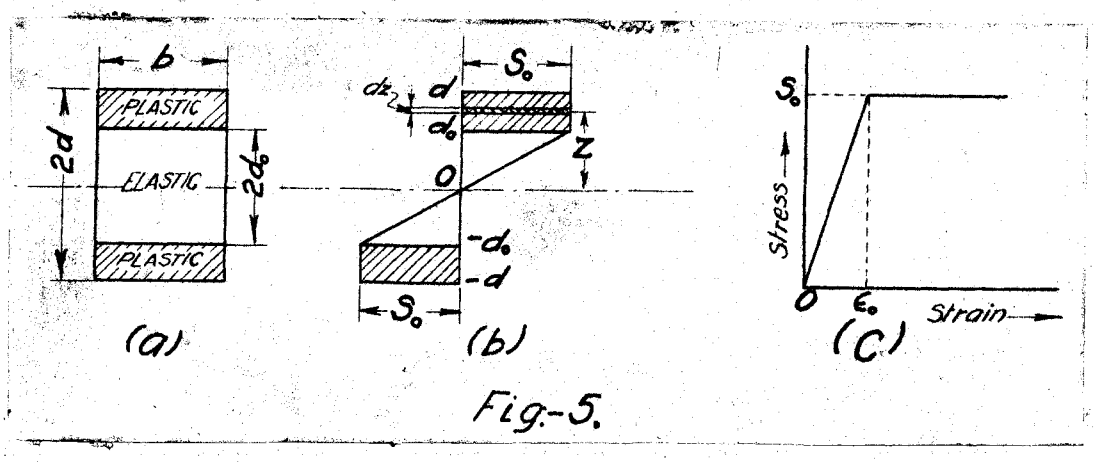

Fig.-5.

From the stress distribution diagram equation for internal moment can be written as the integral over the area of the section

$$M = \int_0^A Szdz$$

$$= b \int_{-d}^{d} Szdz, \qquad (4)$$

where

$$\text{for } 0 \leq z \leq d_0, \quad S = \frac{S_0 z}{d_0}$$

$$\text{for } d_0 \leq z \leq d, \quad S = S_0.$$

Integrating within the limits we can write Eq. 4 as

$$M = b\left[\int_{-d_o}^{d_o} Szdz + \int_{d_o}^{d} S_o z dz + \int_{-d}^{-d_o} S_o z dz\right]$$

$$= b\left[2\int_{0}^{d_o} \frac{S_o z}{d_o} z dz + 2\int_{d_o}^{d} S_o z dz\right]$$

$$= 2b\left[\frac{S_o d_o^3}{3d_o} + \frac{S_o d^2}{2} - \frac{S_o d_o^2}{2}\right]$$

$$= 2bS_o\left[\frac{d^2}{2} - \frac{d_o^2}{6}\right]$$

$$= \frac{2}{3} S_o b d^2 \left[\frac{3}{2} - \frac{1}{2}\left(\frac{d_o}{d}\right)^2\right] \qquad (4a)$$

If we define $\frac{d_o}{d} = u$, Eq. 4a becomes

$$M = \frac{2}{3} S_o b d^2 \left(\frac{3}{2} - \frac{u^2}{2}\right). \qquad (4b)$$

Since $\frac{2}{3} S_o b d^2$ is the maximum moment a rectangular section can develop without going into plastic range of stress. If we substitute $M_o = \frac{2}{3} S_o b d^2$, Eq. 4a reduces to

$$M = M_o \left(\frac{3}{2} - \frac{u^2}{2}\right). \qquad (5)$$

B. Assumptions

In this analysis the following assumptions are made in the development of the equations for the plastic behavior of a flexible ring.

1. The material is isotropic.
2. Deformation of a ring caused by direct tension or compression is negligible.
3. Deflection due to shearing force is negligible.
4. A plane section of a ring before bending remains plane during and after bending beyond the elastic limit.
5. Hooke's Law is valid up to the elastic limit of the material.
6. The idealized stress-strain diagram for pure bending represents the true stress-strain diagram of the material.
7. The moduli of elasticity in tension and compression are equal.
8. A ring is initially circular and of uniform rectangular cross-section.
9. Only a portion of the ring under the load is stressed to the plastic range of stress.
10. The thickness of the ring is small compared to its radius so that the neutral plane can be considered to be passing through its mid-thickness.
11. The free-body at any portion of the ring is in equilibrium under the applied load.

C. Limitations to the Assumptions

Assumption 1 can be said to be generally true for all practical purposes. Assumptions 2 and 3 will be approximately true, only if the thickness of the ring be small compared to its radius, in other words if the ring can be called a thin ring. Assumptions 4 and 5 have been experimentally verified. Assumption 6 is nearly true in the case of soft annealed wrought iron, mild steel, etc., but in the case of material like aluminum alloys it does not hold good. However, assumption 6 still may be desirable in certain type of problems in order to simplify their mathematical solutions. Assumption 7 is found to be true experimentally for the types of metals used in engineering practice. Good workmanship will make assumption 8 reasonably true. Assumption 9 limits the load such that in Fig. 6b the section of the ring at the point A will not be stressed beyond the elastic limit. Assumption 10 is approximately true in the case of thin rings. Assumption 11 will be true if at any instant the plastic flow taking place in any part of the ring be negligible.

D. Development of the Basic Differential Equations

a. Elastic portion of the ring. Fig. 6a shows the ring and the loading condition. The portions of the ring within

angle 2α denotes the regions which are partially in the plastic range of stress. As the loading system is symmetrical with

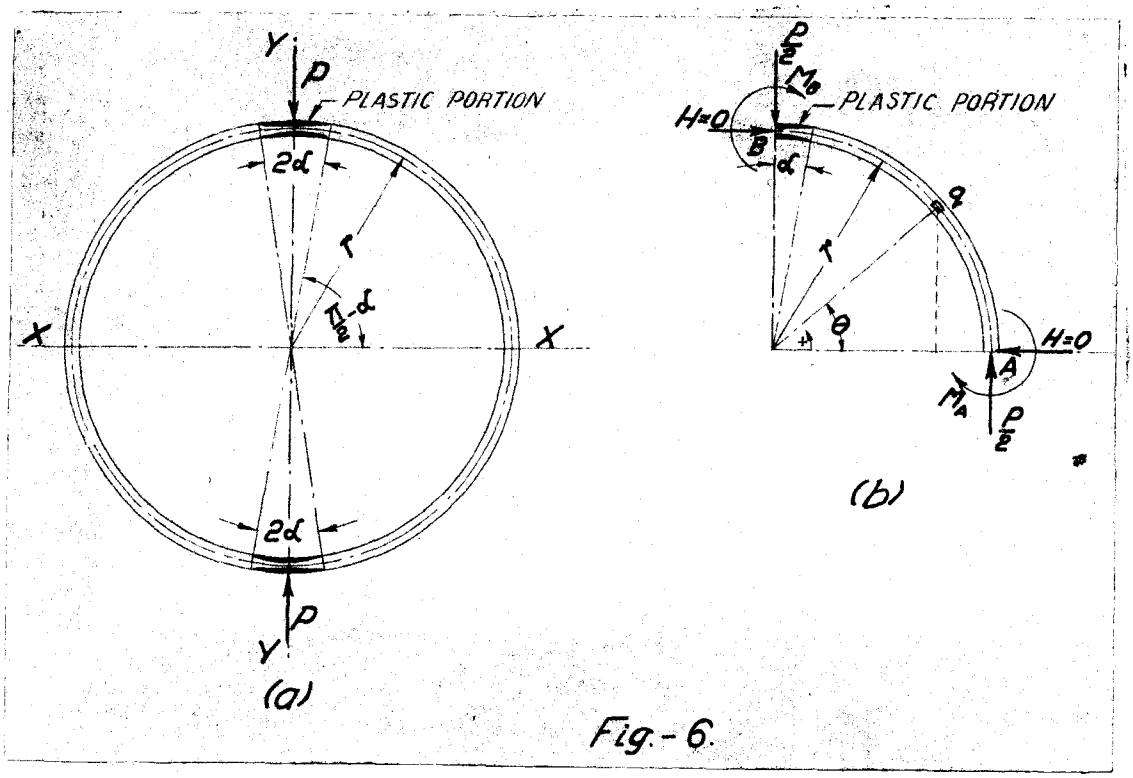

Fig. - 6.

respect to both XX and YY axes this ring problem can be analysed from the free-body diagram of a quarter of the ring. Fig. 6b shows the free-body diagram of a quarter of the ring.

From Fig. 6b the general expression for moment at any point q on the ring, making an angle θ with the horizontal axis, may be written as,

$$M_q = \frac{Pr}{2}(1 - \cos\theta) - M_A. \qquad (6)$$

From the equation of the elastic curve we know,

Change of curvature at any section

$$= \frac{\text{the moment developed at the section}}{\text{flexural rigidity of the section}}.$$

Then we can write at any section of the ring

$$\frac{1}{r} - \frac{1}{\rho} = \frac{M_q}{EI} . \qquad (7)$$

If we put value of $\frac{1}{\rho}$ and M_q from Eqs. 2 and 6, respectively, Eq. 7 reduces to

$$y'' + y = - \frac{r^2}{EI}\left[\frac{Pr}{2}(1-\cos\theta) - M_A\right],$$

or

$$(D^2+1)y = \frac{r^2}{EI}(M_A - \frac{Pr}{2}) + \frac{r^2}{EI}\frac{Pr}{2}\cos\theta. \qquad (8)$$

b. Partially plastic portion of the ring. In Fig. 6b the plastic portion of the ring can be represented by the limit $(\frac{\pi}{2} - \alpha) \leq \theta \leq \frac{\pi}{2}$. The general expression for moment given by Eq. 6 holds true at any point on the ring $0 \leq \theta \leq \frac{\pi}{2}$. The expression for internal moment given by Eq. 5 holds within the limit $(\frac{\pi}{2} - \alpha) \leq \theta \leq \frac{\pi}{2}$. So within the limit $(\frac{\pi}{2} - \alpha) \leq \theta \leq \frac{\pi}{2}$. it may be stated

$$\frac{Pr}{2}(1 - \cos\theta) - M_A = M_0(\frac{3}{2} - \frac{u^2}{2}), \qquad (9)$$

or

$$u^2 = 3 + \frac{2M_A}{M_0} - \frac{Pr}{M_0}(1 - \cos\theta). \qquad (9a)$$

If we put $1 - \cos\theta = 2\sin^2\frac{\theta}{2}$, Eq. 9a becomes

$$u^2 = 3 + \frac{2M_A}{M_o} - \frac{2Pr}{M_o} \sin^2 \frac{\theta}{2} . \qquad (9b)$$

Now letting $3 + \frac{2M_A}{M_o} = R_1$, $\frac{2Pr}{M_o} = R_2$, in Eq. 9b we have

$$u^2 = R_1 - R_2 \sin^2 \frac{\theta}{2} , \qquad (9c)$$

or

$$u = R_1^{\frac{1}{2}} (1 - \frac{R_2}{R_1} \sin^2 \frac{\theta}{2})^{\frac{1}{2}} . \qquad (9d)$$

Now letting $\frac{R_2}{R_1} = N$, in Eq. 9d we have

$$u = R_1^{\frac{1}{2}} (1 - N \sin^2 \frac{\theta}{2})^{\frac{1}{2}} . \qquad (10)$$

It may be noted here that by definition u lies within the limits $0 \leq u \leq 1$. As maximum $\theta = \frac{\pi}{2}$. Then maximum $\sin^2 \frac{\theta}{2} = \frac{1}{2}$. Therefore, in order that Eq. 10 be true, N must be $N \leq 2$. We know $R_1 > 3$, now if N be less than or equal to 1, say N = 1. Then at $\theta = \frac{\pi}{2}$ minimum $u = R_1^{\frac{1}{2}} \times \frac{1}{\sqrt{2}}$ or $u > \sqrt{\frac{3}{2}} > 1$, which is absurd. Hence it can be reasoned that value of N lies within the limits $1 < N \leq 2$.

Figs. 7a, 7b and 7c represent cross-section of the ring portion in plastic range of stress, portion of the ring in plastic range of stress and stress-strain diagram of the ring

material, respectively.

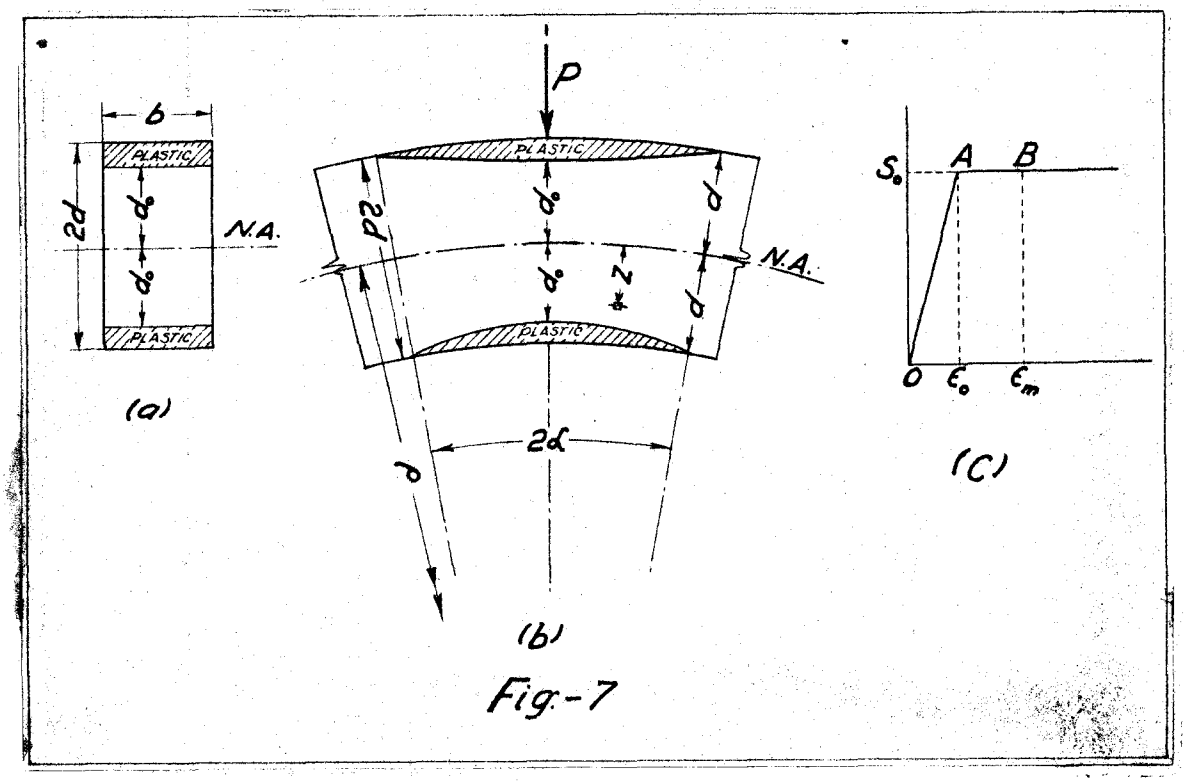

Fig.-7

From geometry (see Eq. 3)

$$\frac{1}{r} - \frac{1}{\rho} = \frac{\epsilon_m}{d} = \frac{\epsilon_0}{d_0} = \frac{\epsilon}{z} . \qquad (3a)$$

In Eq. 3a, $\epsilon_0 = \frac{S_0}{E}$, where ϵ_0 = elastic limit strain, S_0 = elastic limit stress, and E = modulus of elasticity of the material. Using value for ϵ_0 in Eq. 3a we get,

$$\frac{1}{r} - \frac{1}{\rho} = \frac{S_0}{Ed_0} . \qquad (3b)$$

Introducing $u = \frac{d_0}{d}$ and substituting value of $\frac{1}{\rho}$ from Eq. 2, in Eq. 3b we get,

$$\frac{y''}{r^2} + \frac{y}{r^2} = -\frac{S_o}{Ed}\, u^{-1}. \qquad (3c)$$

Letting $\frac{S_o}{Ed} = A$ and taking the value of u from Eq. 10, we can write Eq. 3c as

$$y'' + y = -Ar^2 R_1^{-\frac{1}{2}} (1 - N\sin^2 \tfrac{\theta}{2})^{-\frac{1}{2}}. \qquad (3d)$$

Now letting $-Ar^2 R_1^{-\frac{1}{2}} = Q$ in Eq. 3d we get

$$y'' + y = Q(1 - N \sin^2 \tfrac{\theta}{2})^{-\frac{1}{2}},$$

or

$$(D^2+1)y = Q(1 - N \sin^2 \tfrac{\theta}{2})^{-\frac{1}{2}}. \qquad (11)$$

E. General Solutions of the Differential Equations

a. Elastic portion. The complementary solution of Eq. 8 can be written directly as,

$$y_{comp.} = C_3 \sin\theta + C_4 \cos\theta. \qquad (8a)$$

The particular solution is

$$y_{part.} = \frac{1}{D^2+1}\left[\frac{r^2}{EI}\left(M_A - \frac{Pr}{2}\right) + \frac{r^2}{EI}\frac{Pr}{2}\cos\theta\right]. \qquad (8b)$$

Since $\frac{1}{D^2+1}C = C$, and $\frac{1}{D^2+1}\cos\theta = \frac{1}{2}\theta\sin\theta$, Eq. 8b can be

written as

$$y_{part.} = \frac{r^2}{EI}\left(M_A - \quad\right) + \frac{Pr^3}{4EI}\theta\sin\theta \ . \qquad (8c)$$

If we add Eqs. 8a and 8c, the general solution of Eq. 8 becomes

$$y_e = C_3\sin\theta + C_4\cos\theta + \frac{r^2}{EI}\left(M_A - \frac{Pr}{2}\right) + \frac{Pr^3}{4EI}\theta\sin\theta \ . \qquad (12)$$

In Eq. 12 y_e represents the radial deflection of the ring in its elastic part.

b. Partially plastic portion. As in the elastic portion the complementary solution of Eq. 11 may be written as

$$y_{comp.} = C_1\sin\theta + C_2\cos\theta \ . \qquad (11a)$$

The particular solution is:

$$y_{part.} = \frac{1}{D^2+1}Q\left(1 - N\sin^2\frac{\theta}{2}\right)^{-\frac{1}{2}}, \qquad (11b)$$

or

$$= \frac{1}{2i}\left(\frac{1}{D-i} - \frac{1}{D+i}\right)Q\left(1 - N\sin^2\frac{\theta}{2}\right)^{-\frac{1}{2}},$$

where $i = \sqrt{-1}$

$$= \frac{1}{2i}\left[\frac{1}{D-i}Q\left(1-N\sin^2\frac{\theta}{2}\right)^{-\frac{1}{2}} - \frac{1}{D+i}Q\left(1-N\sin^2\frac{\theta}{2}\right)^{-\frac{1}{2}}\right]$$

$$= \frac{1}{2i}\left[e^{i\theta}\int e^{-i\theta}\frac{Q\,d\theta}{\sqrt{1-N\sin^2\frac{\theta}{2}}} - e^{-i\theta}\int e^{i\theta}\frac{Q\,d}{\sqrt{1-N\sin^2\frac{\theta}{2}}}\right] \qquad (11c)$$

If we substitute $e^{i\theta} = \cos\theta + i\sin\theta$, and $e^{-i\theta} = \cos\theta - i\sin\theta$, Eq. 11c becomes

$$y_{part.} = \frac{Q}{2i}\left[(\cos\theta+i\sin\theta)\int\frac{(\cos\theta-i\sin\theta)}{\sqrt{1-N\sin^2\frac{\theta}{2}}}\,d\theta - (\cos\theta-i\sin\theta)\int\frac{(\cos\theta+i\sin\theta)}{\sqrt{1-N\sin^2\frac{\theta}{2}}}\,d\theta\right]$$

or

$$y_{part.} = Q\left[\sin\theta\int\frac{\cos\theta d\theta}{\sqrt{1-N\sin^2\frac{\theta}{2}}} - \cos\theta\int\frac{\sin\theta d\theta}{\sqrt{1-N\sin^2\frac{\theta}{2}}}\right], \qquad (11d)$$

Second integral of Eq. 11d.

$$\int\frac{\sin\theta d\theta}{\sqrt{1-N\sin^2\frac{\theta}{2}}} = \frac{4}{N}\int\frac{N\sin\frac{\theta}{2}\cos\frac{\theta}{2}}{\sqrt{1-N\sin^2\frac{\theta}{2}}}\,d\frac{\theta}{2}$$

and

$$d\sqrt{1-N\sin^2\frac{\theta}{2}} = -\frac{N\sin\frac{\theta}{2}\cos\frac{\theta}{2}}{\sqrt{1-N\sin^2\frac{\theta}{2}}}\,d\frac{\theta}{2}.$$

Therefore,

$$\int\frac{\sin\theta d\theta}{\sqrt{1-N\sin^2\frac{\theta}{2}}} = -\frac{4}{N}\sqrt{1-N\sin^2\frac{\theta}{2}}\,. \qquad (a)$$

First integral of Eq. 11d.

$$\int \frac{\cos\theta d\theta}{\sqrt{1-N\sin^2\frac{\theta}{2}}} = \int \frac{(1-2\sin^2\frac{\theta}{2})}{\sqrt{1-N\sin^2\frac{\theta}{2}}} 2d\frac{\theta}{2}$$

or

$$= 2\left[\int \frac{d\frac{\theta}{2}}{\sqrt{1-N\sin^2\frac{\theta}{2}}} - 2\int \frac{\sin^2\frac{\theta}{2}d\frac{\theta}{2}}{\sqrt{1-N\sin^2\frac{\theta}{2}}}\right] \quad (b)$$

Substituting $\sin^2\frac{\theta}{2} = \frac{1}{N} - \frac{1}{N}(1-N\sin^2\frac{\theta}{2})$ in Eq. b, we get,

$$\int \frac{\cos\theta d\theta}{\sqrt{1-N\sin^2\frac{\theta}{2}}} = 2\left[(1-\frac{2}{N})\int \frac{d\frac{\theta}{2}}{\sqrt{1-N\sin^2\frac{\theta}{2}}} + \frac{2}{N}\int \sqrt{1-N\sin^2\frac{\theta}{2}}\ d\frac{\theta}{2}\right] \quad (b_1)$$

It has been shown before that N is $1 < N \leq 2$. Hence in order that Eq. C may be transformed into elliptic integral form, change of variable is necessary.

Let

$$N\sin^2\frac{\theta}{2} = \sin^2\phi,$$

then

$$\frac{\theta}{2} = \sin^{-1}(\frac{1}{N}\sin\phi),$$

or

$$d\frac{\theta}{2} = \frac{1}{N}\frac{\cos\phi d\phi}{\sqrt{1-\frac{1}{N}\sin^2\phi}}.$$

Using the above substitutions we can write

$$\int \frac{d\frac{\theta}{2}}{\sqrt{1-N\sin^2\frac{\theta}{2}}} = \frac{1}{\sqrt{N}}\int \frac{\cos\phi d\phi}{\sqrt{1-\sin^2\phi}\ \sqrt{1-\frac{1}{N}\sin^2\phi}} ,$$

or

$$= \frac{1}{\sqrt{N}}\int \frac{d\phi}{\sqrt{1-\frac{1}{N}\sin^2\phi}} . \qquad (c)$$

Similarly

$$\int \sqrt{1-N\sin^2\frac{\theta}{2}}\, d\frac{\theta}{2} = \frac{1}{\sqrt{N}}\int \frac{d\phi}{\sqrt{1-\frac{1}{N}\sin^2\phi}} - \frac{1}{\sqrt{N}}\int \frac{\sin^2\phi\, d\phi}{\sqrt{1-\frac{1}{N}\sin^2\phi}} . \qquad (d)$$

If we substitute $\sin^2\phi = N-N(1-\frac{1}{N}\sin^2\phi)$, Eq. d becomes

$$\int \sqrt{1-N\sin^2\frac{\theta}{2}}\, d\frac{\theta}{2} = \frac{(1-N)}{\sqrt{N}}\int \frac{d\phi}{\sqrt{1-\frac{1}{N}\sin^2\phi}} + \sqrt{N}\int \sqrt{1-\frac{1}{N}\sin^2\phi}\ d\phi . \qquad (d_1)$$

If we substitute values from Eqs. c and d_1, Eq. b_1 becomes:

$$\int \frac{\cos\theta d\theta}{\sqrt{1-N\sin^2\frac{\theta}{2}}} = \frac{2}{\sqrt{N}}\left[2\int \sqrt{1-\frac{1}{N}\sin^2\phi}\ d\phi - \int \frac{d\phi}{\sqrt{1-\frac{1}{N}\sin^2\phi}}\right] . \qquad (b_2)$$

Right hand side of Eq. b_2 now is in elliptic integral form. The limits of the elliptic integrals can be determined as follows:

Plastic stress in the ring exists for values of Θ in $(\frac{\pi}{2}-\alpha) \leq \theta \leq \frac{\pi}{2}$. So the limits of integration will be $(\frac{\pi}{2}-\alpha)$ and θ , θ being the upper limit of the integrals. When the variable of integration is $\frac{\theta'}{2}$ limits of the integrals become $(\frac{\pi}{2}-\alpha)$ and $\frac{\theta}{2}$, $\frac{\theta}{2}$ being the upper limit.

Now if we let

$$N \sin^2\frac{\theta'}{2} = \sin^2\phi.$$

Then

$$\text{for } \frac{\theta'}{2} = \frac{\theta}{2}, \quad \phi = \sin^{-1}(\sqrt{N} \sin\frac{\theta}{2})$$

$$\text{fpr } \frac{\theta'}{2} = (\frac{\pi}{2}-\frac{\alpha}{2}), \quad \phi = \sin^{-1}\left[\sqrt{N} \sin(\frac{\pi}{4}-\frac{\alpha}{2})\right].$$

Putting in the limits of integration, we can write Eq. b_2 as

$$\int_{(\frac{\pi}{2}-\alpha)}^{\theta} \frac{\cos\theta' d\theta'}{\sqrt{1-N \sin^2\frac{\theta'}{2}}} = 2 \int_{(\frac{\pi}{4}-\frac{\alpha}{2})}^{\frac{\theta}{2}} \frac{\cos\theta' d\frac{\theta'}{2}}{\sqrt{1-N \sin^2\frac{\theta'}{2}}}$$

or

$$= \frac{2}{\sqrt{N}}\left[2 \int_{\sin^{-1}\left\{\sqrt{N} \sin(\frac{\pi}{4}-\frac{\alpha}{2})\right\}}^{\sin^{-1}(\sqrt{N} \sin\frac{\theta}{2})} \frac{d\phi}{\sqrt{1-\frac{1}{N} \sin^2\phi}} - \int_{\sin^{-1}\left\{\sqrt{N} \sin(\frac{\pi}{4}-\frac{\alpha}{2})\right\}}^{\sin^{-1}(\sqrt{N} \sin\frac{\theta}{2})} \frac{d\phi}{\sqrt{1-\frac{1}{N}\sin^2\phi}}\right] \quad (b_3)$$

As the lower limit of the integrals is a constant the value obtained from the lower limit can be absorbed in constants C_1 and C_2 of Eq. 11a. Then Eq. b can be written as,

$$\int_0^{\theta} \frac{\cos\theta' d\theta'}{\sqrt{1-N\sin^2\frac{\theta'}{2}}} = \frac{2}{\sqrt{N}}\left[2\int_0^{\sin^{-1}(\sqrt{N}\sin\frac{\theta}{2})} \sqrt{1-\frac{1}{N}\sin^2\phi}\; d\phi - \int_0^{\sin^{-1}(\sqrt{N}\sin\frac{\theta}{2})} \frac{d\phi}{\sqrt{1-\frac{1}{N}\sin^2\phi}}\right]$$

or

$$= \frac{2}{\sqrt{N}}\left[2E\left\{\frac{1}{\sqrt{N}}, \sin^{-1}(\sqrt{N}\sin\frac{\theta}{2})\right\} - F\left\{\frac{1}{\sqrt{N}}, \sin^{-1}(\sqrt{N}\sin\frac{\theta}{2})\right\}\right]. \qquad (b_4)$$

If we take values from Eqs. a and b_4, Eq. 11d can be written as,

$$y_{part.} = Q\sin\theta\frac{2}{\sqrt{N}}\left[2E\left\{\frac{1}{\sqrt{N}}, \sin^{-1}(\sqrt{N}\sin\frac{\theta}{2})\right\} - F\left\{\frac{1}{\sqrt{N}}, \sin^{-1}(\sqrt{N}\sin\frac{\theta}{2})\right\}\right] + \frac{4Q\cos\theta}{N}\sqrt{1-N\sin^2\frac{\theta}{2}}. \qquad (11e)$$

If we add Eqs. 11a and 11e, the general solution of Eq. 11 becomes:

$$y_p = C_1 \sin\theta + C_2 \cos\theta + \frac{40\sin\theta}{\sqrt{N}} E\left\{\frac{1}{\sqrt{N}}, \sin^{-1}(\sqrt{N}\sin\frac{\theta}{2})\right\}$$

$$- \frac{20\sin\theta}{\sqrt{N}} F\left\{\frac{1}{\sqrt{N}}, \sin^{-1}(\sqrt{N}\sin\frac{\theta}{2})\right\} + \frac{40\cos\theta}{N}\sqrt{1-N\sin^2\frac{\theta}{2}}. \quad (13)$$

In Eq. 13 y_p represents the radial deflection of the ring in its plastic part. E and F represent 2nd and 1st type of elliptic integral, respectively.

F. The Unknown Constants

The unknown constants in this analysis are:

1. M_A, the moment at the point A.
2. C_1, the coefficient of $\sin\theta$ in Eq. 13.
3. C_2, the coefficient of $\cos\theta$ in Eq. 13.
4. C_3, the coefficient of $\sin\theta$ in Eq. 12.
5. C_4, the coefficient of $\cos\theta$ in Eq. 12.
6. α, the measure of the plastic portion of the ring (see Figs. 6a and 6b).

G. The Boundary Conditions

The boundary conditions in this analysis are:

1. At $\theta = \frac{\pi}{2}$, $\frac{dy_p}{d\theta} = 0$.
2. At $\theta = 0$, $\frac{dy_e}{d\theta} = 0$.
3. At $\theta = (\frac{\pi}{2} - \alpha)$, $u = 1$.

4. At $\theta = (\frac{\pi}{2}-\alpha)$, $y_p = y_e$ i.e. Elasto-plastic deflection = elastic deflection.

5. At $\theta = (\frac{\pi}{2}-\alpha)$, $\frac{dy_p}{d\theta} = \frac{dy_e}{d\theta}$ i.e. Elasto-plastic slope = elastic slope.

6. At $\theta = (\frac{\pi}{2}-\alpha)$, $\frac{d^2y_p}{d\theta^2} = \frac{d^2y_e}{d\theta^2}$ i.e. Elasto-plastic curvature = elastic curvature.

H. Determination of the Constants

Boundary condition no. 3 states, at $\theta = \frac{\pi}{2} - \alpha$, $u = 1$. In Eq. 9a substituting the boundary condition no. 3, we get

$$1 = 3 + \frac{2M_A}{M_o} - \frac{Pr}{M_o}(1-\sin\alpha). \qquad (14)$$

Simplification of Eq. 14 yields:

$$M_A = \frac{Pr}{2}(1-\sin\alpha) - M_o. \qquad (15)$$

Using the value of M_A from Eq. 15 we can have

$$R_1 = 1 + \frac{Pr}{M_o}(1-\sin\alpha). \qquad (16)$$

Boundary condition no. 1 states: at $\theta = \frac{\pi}{2}$, $\frac{dy_p}{d\theta} = 0$. Differentiating Eq. 13 with respect to θ we have:

$$\frac{dy_p}{d\theta} = C_1\cos\theta - C_2\sin\theta + \frac{40\cos\theta}{\sqrt{N}} E\left\{\frac{1}{\sqrt{N}}, \sin^{-1}(\sqrt{N}\sin\frac{\theta}{2})\right\}$$

$$- \frac{20\cos\theta}{\sqrt{N}} F\left\{\frac{1}{\sqrt{N}}, \sin^{-1}(\sqrt{N}\sin\frac{\theta}{2})\right\} - \frac{40\sin\theta}{N}\sqrt{1-N\sin^2\frac{\theta}{2}} \quad (17)$$

At $\theta = \frac{\pi}{2}$,

$$\frac{dy_p}{d\theta} = - C_2 - \frac{40}{N}\sqrt{1-\frac{N}{2}} = 0$$

or

$$C_2 = - \frac{40}{N}\sqrt{1-\frac{N}{2}} \; . \quad (18)$$

Boundary condition no. 2 states: at $\theta = 0$, $\frac{dy_e}{d\theta} = 0$. Differentiating Eq. 12 with respect to θ we get,

$$\frac{dy_e}{d\theta} = C_3\cos\theta - C_4\sin\theta + \frac{Pr^3}{4EI}(\sin\theta + \cos\theta). \quad (19)$$

At $\theta = 0$,

$$\frac{dy_e}{d\theta} = C_3 = 0,$$

or

$$C_3 = 0. \quad (20)$$

Boundary condition no. 4 states: at $\theta = (\frac{\pi}{2}-\alpha)$, $y_p = y_e$. At $\theta = (\frac{\pi}{2}-\alpha)$ equating Eqs. 13 and 12, and substituting values

of C_2 and C_3 from Eqs. 18 and 20, we have:

$$C_1\cos\alpha - \frac{4Q}{N}\sqrt{1-\frac{N}{2}}\sin\alpha + \frac{4Q\cos\alpha}{\sqrt{N}} E\left[\frac{1}{\sqrt{N}}, \sin^{-1}\left\{\sqrt{N}\sin\left(\frac{\pi}{4}-\frac{\alpha}{2}\right)\right\}\right]$$

$$- \frac{2Q\cos\alpha}{\sqrt{N}} F\left[\frac{1}{\sqrt{N}}, \sin^{-1}\left\{\sqrt{N}\sin\left(\frac{\pi}{4}-\frac{\alpha}{2}\right)\right\}\right]$$

$$+ \frac{4Q\sin\alpha}{N}\sqrt{1-N\sin^2\left(\frac{\pi}{4}-\frac{\alpha}{2}\right)} = C_4\sin\alpha + \frac{r^2}{EI}\left(M_A-\frac{Pr}{2}\right)$$

$$+ \frac{Pr^3}{4EI}\left(\frac{\pi}{2}-\alpha\right)\cos\alpha,$$

or

$$C_1\cos\alpha - \frac{4Q}{N}\sqrt{1-\frac{N}{2}}\sin\alpha + \frac{4Q\cos\alpha}{\sqrt{N}} E\left[\frac{1}{\sqrt{N}}, \sin^{-1}\left\{\sqrt{N}\sin\left(\frac{\pi}{4}-\frac{\alpha}{2}\right)\right\}\right]$$

$$- \frac{2Q\cos\alpha}{\sqrt{N}} F\left[\frac{1}{\sqrt{N}}, \sin^{-1}\left\{\sqrt{N}\sin\left(\frac{\pi}{4}-\frac{\alpha}{2}\right)\right\}\right]$$

$$+ \frac{4Q\sin\alpha}{N}\sqrt{1-N\sin^2\left(\frac{\pi}{4}-\frac{\alpha}{2}\right)} - C_4\sin\alpha - \frac{r^2}{EI}\left(M_A-\frac{Pr}{2}\right)$$

$$- \frac{Pr^3}{4EI}\left(\frac{\pi}{2}-\alpha\right)\cos\alpha = 0. \qquad (21)$$

Boundary condition no. 5 states: at $\theta = \left(\frac{\pi}{2}-\alpha\right)$, $\frac{dy_p}{d\theta} = \frac{dy_e}{d\theta}$. At $\theta = \left(\frac{\pi}{2}-\alpha\right)$ equating Eqs. 17 and 19 and substituting values of C_2 and C_3 as before, we get

$$C_1\sin\alpha + \frac{4Q}{N}\sqrt{1-\frac{N}{2}}\cos\alpha + \frac{4Q\sin\alpha}{\sqrt{N}}\,E\left[\frac{1}{\sqrt{N}},\sin^{-1}\left\{\sqrt{N}\,\sin\left(\frac{\pi}{4}-\frac{\alpha}{2}\right)\right\}\right]$$

$$-\frac{2Q\sin\alpha}{\sqrt{N}}\,F\left[\frac{1}{\sqrt{N}},\sin^{-1}\left\{\sqrt{N}\,\sin\left(\frac{\pi}{4}-\frac{\alpha}{2}\right)\right\}\right]$$

$$-\frac{4Q\cos\alpha}{N}\sqrt{1-N\sin^2\left(\frac{\pi}{4}-\frac{\alpha}{2}\right)} + C_4\cos\alpha - \frac{Pr^3}{4EI}\left(\frac{\pi}{2}-\alpha\right)\sin\alpha$$

$$-\frac{Pr^3}{4EI}\cos\alpha = 0. \qquad (22)$$

Boundary condition no. 6 gives rise to an identity, so in order to determine all the unknown constants we will have to use an extra condition not included in the boundary conditions which is,

At any section of the ring, external moment is equal in magnitude to the internal resisting moment.

Multiplying Eq. 21 by sinα we get,

$$C_1\cos\alpha\sin\alpha - \frac{4Q}{N}\sqrt{1-\frac{N}{2}}\sin^2\alpha + \frac{4Q\cos\alpha\sin\alpha}{\sqrt{N}}E\left[\frac{1}{\sqrt{N}}\sin^{-1}\left\{\sqrt{N}\,\sin\left(\frac{\pi}{4}-\frac{\alpha}{2}\right)\right\}\right]$$

$$-\frac{2Q\cos\alpha\sin\alpha}{\sqrt{N}}F\left[\frac{1}{\sqrt{N}}\sin^{-1}\left\{\sqrt{N}\,\sin\left(\frac{\pi}{4}-\frac{\alpha}{2}\right)\right\}\right]$$

$$+\frac{4Q\sin^2\alpha}{N}\sqrt{1-N\sin^2\left(\frac{\pi}{4}-\frac{\alpha}{2}\right)} - C_4\sin^2\alpha$$

$$-\frac{r^2}{EI}\left(M_A-\frac{Pr}{2}\right)\sin\alpha - \frac{Pr^3}{4EI}\left(\frac{\pi}{2}-\alpha\right)\cos\alpha\sin\alpha = 0. \qquad (21a)$$

Also multiplying Eq. 22 by cosα we get,

$$C_1 \sin\alpha\cos\alpha + \frac{4Q}{N}\sqrt{1-\frac{N}{2}}\,\cos^2\alpha + \frac{4Q\cos\alpha\sin\alpha}{\sqrt{N}}E\left[\frac{1}{\sqrt{N}}\sin^{-1}\left\{\sqrt{N}\,\sin\left(\frac{\pi}{4}-\frac{\alpha}{2}\right)\right\}\right]$$

$$-\frac{2Q\sin\alpha\cos\alpha}{\sqrt{N}}F\left[\frac{1}{\sqrt{N}}\sin^{-1}\left\{\sqrt{N}\,\sin\left(\frac{\pi}{4}-\frac{\alpha}{2}\right)\right\}\right]$$

$$-\frac{4Q\cos^2\alpha}{N}\sqrt{1-N\sin^2\left(\frac{\pi}{4}-\frac{\alpha}{2}\right)} + C_4\cos^2\alpha - \frac{Pr^3}{4EI}\cos^2\alpha$$

$$-\frac{Pr^3}{4EI}\left(\frac{\pi}{2}-\alpha\right)\sin\alpha\cos\alpha = 0. \qquad (22a)$$

Now subtracting Eq. 21a from Eq. 22a and substituting value of M_A from Eq. 15 we have

$$C_4 = \frac{4Q}{N}\left\{\sqrt{1-N\,\sin^2\left(\frac{\pi}{4}-\frac{\alpha}{2}\right)} - \sqrt{1-\frac{N}{2}}\right\} + \frac{Pr^3}{4EI}\left(1+\sin^2\alpha\right) + \frac{M_o r^2}{EI}\sin\alpha. \qquad (23)$$

Similarly, multiplying Eq. 21 by $\cos\alpha$ and Eq. 22 by $\sin\alpha$, then subtracting one from the other we get

$$C_1 = \frac{2Q}{\sqrt{N}}\left[F\left\{\frac{1}{\sqrt{N}}\sin^{-1}\left\{\sqrt{N}\,\sin\left(\frac{\pi}{4}-\frac{\alpha}{2}\right)\right\}\right\} - 2E\left\{\frac{1}{\sqrt{N}}\sin^{-1}\left\{\sqrt{N}\,\sin\left(\frac{\pi}{4}-\frac{\alpha}{2}\right)\right\}\right\}\right]$$

$$+\frac{Pr^3}{4EI}\left\{\left(\frac{\pi}{2}-\alpha\right) - \cos\alpha\sin\alpha\right\} - \frac{M_o r^2}{EI}\cos\alpha. \qquad (24)$$

From Eq. 6, M_B (see Fig. 6b) can be expressed as

$$M_B = \frac{Pr}{2} - M_A. \qquad (6a)$$

Using value of M_A from Eq. 15 we can write Eq. 6a as

$$M_B = \frac{Pr}{2} \sin\alpha + M_0. \qquad (6b)$$

Now if we equate the external moment M_B at the point B (see Fig. 6b), which can be found approximately, to the right hand side of the Eq. 6b, where Pr and M_0 are known, the value of α can be calculated.

I. Modifications of Moment Equations for the Ring Due to the Change in its Geometry Under Load

By the theory of elastic deformation, the well known equations for the horizontal and vertical radial deflection of a circular ring acting under two equal and opposite concentrated line loads are given by

$$\Delta_x(\text{horiz.}) = .0683 \frac{Pr^3}{EI} \qquad (25)$$

$$\Delta_y(\text{vert.}) = .0744 \frac{Pr^3}{EI}. \qquad (26)$$

Equations 25 and 26 very obviously represent a straight line relationship between load and deflection. In the derivation of these equations it is assumed that the geometry of the ring under the load does not change appreciably to cause

any change in the general moment equation. In other words it is assumed that the moment developed at any section of the ring is proportional to the applied load.

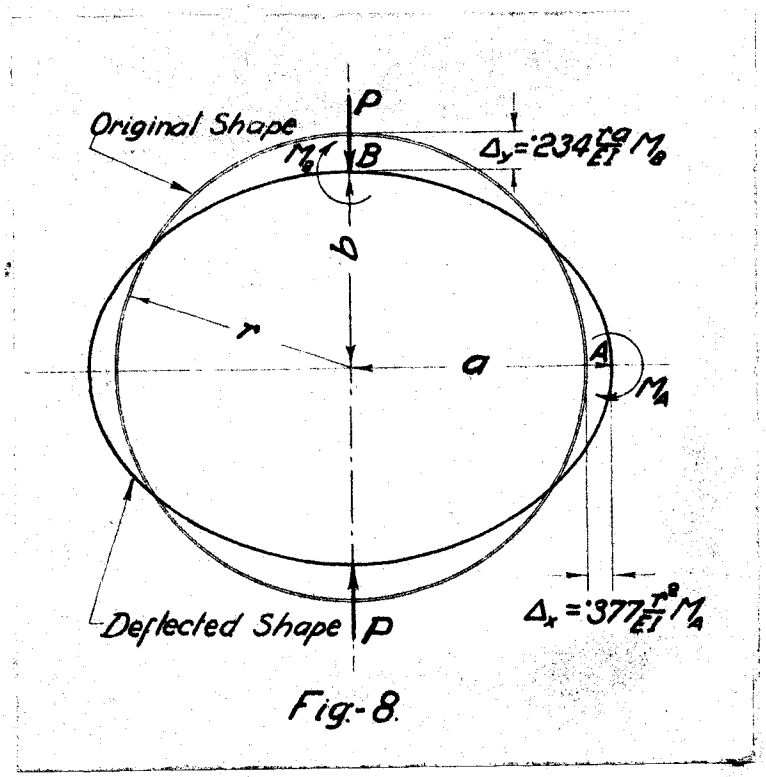

Fig.-8.

If Eqs. 25 and 26 which represent radial deflections at the points A and B be expressed in terms of the moments developed at those points, they become

$$\Delta_x = .377 \frac{r^2}{EI} M_A, \qquad (25a)$$

$$\Delta_y = .234 \frac{r^2}{EI} M_B. \qquad (26a)$$

In order that the effect of the change in geometry of the ring can be taken care of (see Fig. 8), slight modification in Eq. 26a is introduced by replacing r^2 by ra.

Then Eq. 26a becomes:

$$\Delta_y = .234 \frac{Pa}{EI} M_B. \qquad (26b)$$

Though the Eq. 26b is not derived mathematically, it gives closer results to the experimental data than that obtained from Eqs. 25 and 26.

W. F. Burke (3) has developed some curves from which M_A and M_B of a ring may be determined when acting under two equal and opposite concentrated line loads, when the deformed ring is considered to be elliptical (see Fig. 9) and stressed within the elastic limit.

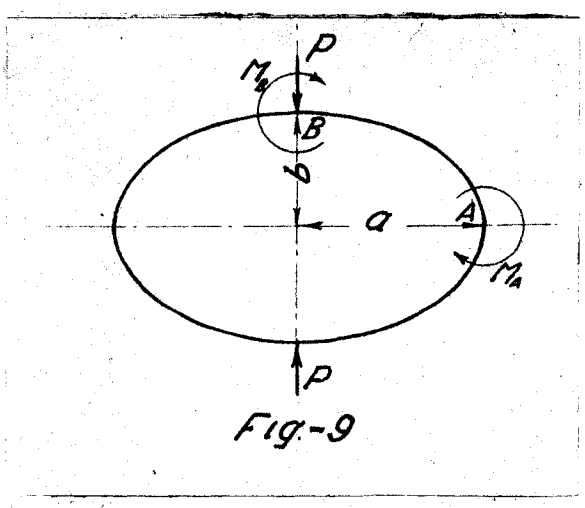

Fig.-9

Table 1

From Burke's graph

$M_A = kaP$	
a/b	k
1.0	.182
1.1	.186
1.3	.195
1.5	.203
1.7	.208
1.9	.213
2.1	.217
2.3	.220
2.5	.223

Burke's formula:

$$M_A = kaP \qquad (27)$$

$$M_B = \frac{Pa}{2} - M_A = Pa(\tfrac{1}{2}-k). \qquad (28)$$

The first approximation for a and b can be obtained as

$$a = r + \Delta_x \text{ and } b = r - \Delta_y,$$

where Δ_x and Δ_y can be obtained from Eqs. 25 and 26. Then from Eqs. 27 and 28, M_A and M_B can be obtained and finally Δ_x and Δ_y can be calculated from Eqs. 25a and 26b. It may be noted here that Δ_x and Δ_y according to our previous notation, essentially represent y at 0^0 and y at 90^0. For a better approximation the operation may be repeated.

From Eq. 15 we know

$$M_A = \frac{Pr}{2}(1-\sin\alpha) - M_0, \quad \text{when } P > P_0;$$

P_0 being the load which stresses the ring section at the point B (see Fig. 6) to its elastic limit.

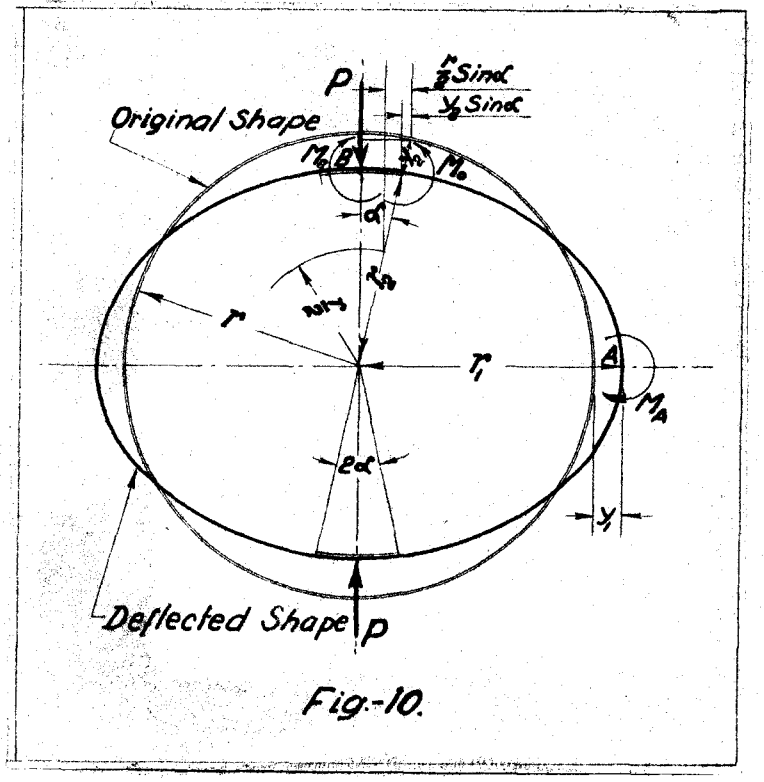

Fig.-10.

From Fig. 10 considering the deflected position of the ring M_A can be written as

$$M_A = \frac{P}{2}(r_1 - r_2 \sin\alpha) - M_0. \qquad (29)$$

In Eq. 29, $r_1 = r + y_1$, $r_2 = r - y_2$. If we put these values of r_1 and r_2, Eq. 29 becomes:

$$M_A = \frac{P}{2}(r+y_1) - \frac{P}{2}(r-y_2)\sin\alpha - M_0,$$

or

$$= \frac{Pr}{2}(1-\sin\alpha) - M_0 + \frac{P}{2}(y_1+y_2\sin\alpha). \qquad (29a)$$

Comparison of Eqs. 15 and 29a shows that the change in geometry of the ring due to the load causes an increment of $\frac{P}{2}(y_1+y_2\sin\alpha)$ in M_A. As both y_1 and y_2 are unknown, an empirical substitution is made as

$$y_1 + y_2\sin\alpha = \frac{r}{2}\sin\alpha. \qquad (30)$$

Though the substitution represented by Eq. 30 is not derived from any theory, it gives a close result compared to the experimental work done by Burke (3).

Using substitution from Eq. 30 in Eq. 29a, we get

$$M_A = \frac{Pr}{2}(1-\sin\alpha) - M_0 + \frac{Pr}{4}\sin\alpha,$$

or

$$M_A = \frac{Pr}{2}(1-\frac{1}{2}\sin\alpha) - M_0. \qquad (31)$$

III. COMPARISONS OF THE THEORETICAL SOLUTIONS WITH RESULTS ON TESTS ON CORRUGATED METAL PIPES

As the theoretical solution has been obtained essentially for a thin circular ring with rectangular section, for the sake of comparison the test data on corrugated pipes were imagined to be from a circular ring with rectangular section, whose moment of inertia of the section and mean radius is same as that of the corrugated pipe. The basic properties of the imaginary ring, such as P_0 and $\frac{r}{EI}$, in every case, were obtained from the graph plotted from the test data of the corresponding corrugated pipe. Width of the ring in each case was considered to be unity.

A. Corrugated pipe of 36 in. nominal diameter; .1094 in. plate thickness; corrugations having 2 2/3 in. pitch and 1/2 in. depth.

The average radius of the ring, r = 18.5 in.

The elastic limit load from Fig. 11a, P_0 = 100 lbs.

By elastic deformation theory,

$$M_A = .1817\ Pr \tag{32}$$

$$M_B = \frac{1}{\pi} Pr. \tag{33}$$

From Eq. 33 we can say,

$$M_o = \frac{P_o r}{\pi} . \qquad (33a)$$

Using Eq. 33a we get, M_o = 590 lb. in.

From Fig. 11a the vertical deflection of the ring Δ_y by elastic deformation theory is .59 in.

Using Eq. 26 we get

$$.0744 \frac{r}{EI} r^2 P_o = .59.$$

Then

$$\frac{r}{EI} = .000231, \qquad \frac{M_o r^2}{EI} = Ar^2 = 2.52$$

$$\frac{r^2}{EI} = .00428 , \qquad \frac{r^3}{4EI} = .0198.$$

From Eq. 6b we have

$$M_B = \frac{Pr}{2} \sin\alpha + M_o.$$

From Eq. 33a we have

$$P_o = \frac{M_o \pi}{r} .$$

From Table 2 when $P = 1.05\ P_o$, $M_B = 1.07\ M_o$. Using conditions of Eqs. 6b and 33a we have

$$1.07\ M_o = \frac{1.05\ M_o \pi r}{2r} \sin\alpha + M_o$$

or

$$\sin\alpha = .0425,$$

or

$$\alpha = 2^o - 26'.$$

Similarly the rest of the αs in Table 2 were calculated.

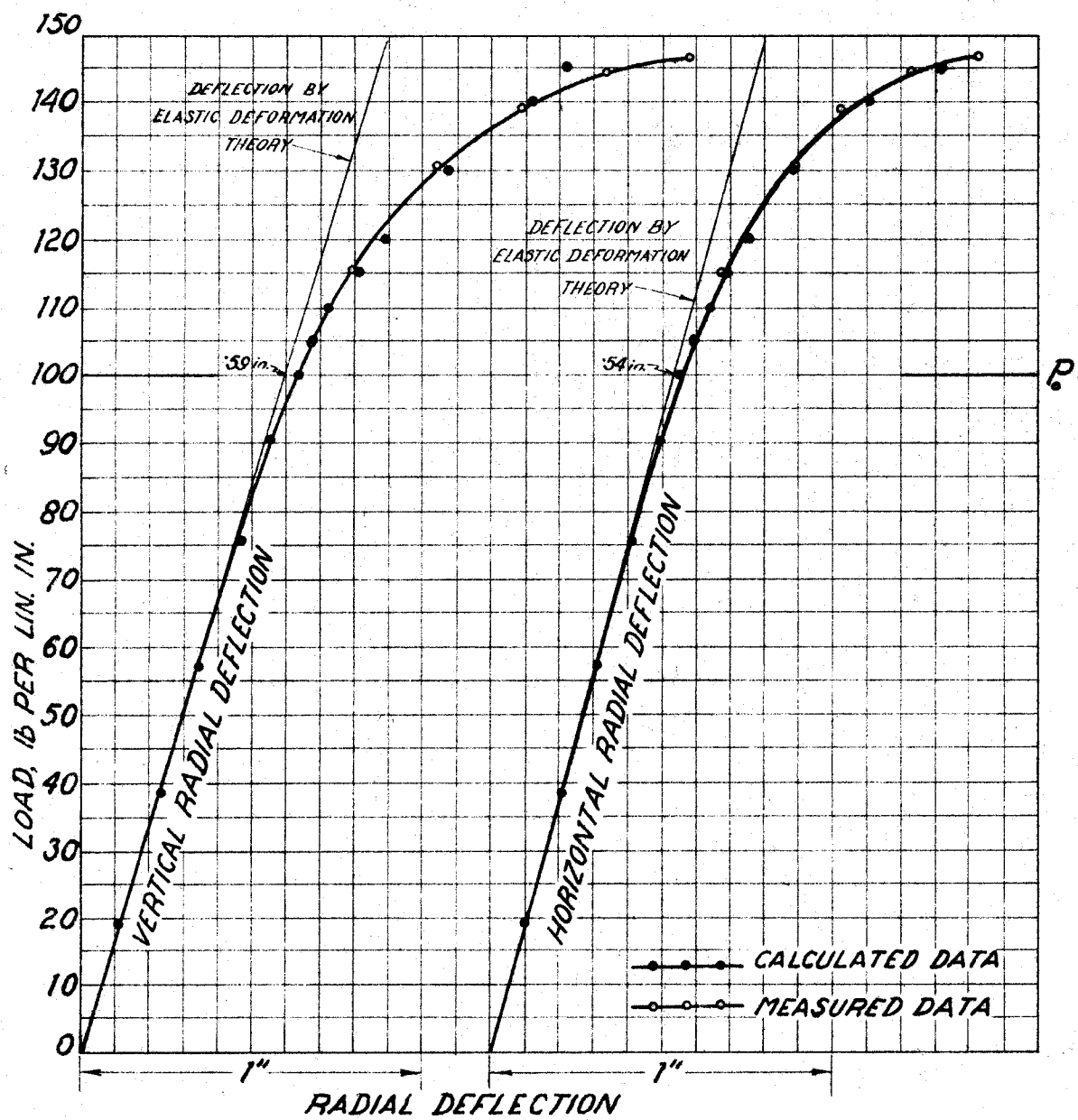
150
140
130
120
110
100
90
80
70
60
50
40
30
20
10
0
LOAD, lb PER LIN. IN.
DEFLECTION BY ELASTIC DEFORMATION THEORY
.59 in.
VERTICAL RADIAL DEFLECTION
DEFLECTION BY ELASTIC DEFORMATION THEORY
.54 in.
HORIZONTAL RADIAL DEFLECTION
P
CALCULATED DATA
MEASURED DATA
1"
1"
RADIAL DEFLECTION

Fig.-11A.

Table 2

	By elastic deformation theory								
P	M_A	M_B	a	b	a/b	k*	M_A**	M_B***	α
0	0	0	18.50	18.50	1	.182	0	0	
19.05	64.2	112	18.60	18.39	1.010	.1824	64.6	112.5	
38.5	130	227	18.71	18.27	1.025	.1830	132	228	
57.0	192	336	18.81	18.16	1.035	.1834	197	340	
75.5	254	445	18.91	18.05	1.050	.1840	263	451	
90.3	304	532	18.99	17.97	1.058	.1843	316	540	
$100=P_o$	337	589	19.04	17.91	1.063	.1845	351	600	
$105=1.05P_o$	354	619	19.07	17.88	1.068	.1847	370	$631=1.07M_o$	$2^o-26'$
$110=1.10P_o$	370	648	19.10	17.85	1.070	.1848	388	$661=1.124M_o$	$4^o-8'$
$115=1.15P_o$	388	678	19.12	17.82	1.074	.1850	407	$692=1.175M_o$	$5^o-34'$
$120=1.20P_o$	404	707	19.15	17.79	1.078	.1851	425	$724=1.23M_o$	$7^o-2'$
$130=1.30P_o$	438	766	19.20	17.73	1.083	.1853	462	$785=1.333M_o$	$9^o-26'$
$140=1.40P_o$	472	825	19.26	17.67	1.090	.1856	500	$850=1.442M_o$	$11^o-36'$
$145=1.45P_o$	488	855	19.28	17.64	1.094	.1858	519	$879=1.492M_o$	$12^o-30'$

* From Table 1

** By Eq. 27

*** By Eq. 28

Table-3.

P	α	$\cos\alpha$	$\sin\alpha$	$\sin^2\alpha$	$\sin(\frac{\pi}{4}-\frac{\alpha}{2})$	$\sin^2(\frac{\pi}{4}-\frac{\alpha}{2})$	$(\frac{\pi}{2}-\alpha)$	$R_1=1+\frac{P_r}{M_\infty^2}(1-\sin\alpha)$	$R_2=\frac{2P_r}{M_\infty}$	$N=\frac{R_2}{R_1}$
$1.05P_r$	2°-26′	.9991	.0425	.00181	.6919	.4787	1.528	4.160	6.60	1.588
$1.10P_r$	4°-8′	.9974	.0721	.0052	.6812	.4640	1.499	4.205	6.91	1.626
$1.15P_r$	5°-34′	.9953	.0970	.00941	.6719	.4515	1.474	4.260	7.23	1.698
$1.20P_r$	7°-2′	.9925	.1222	.01493	.6624	.4388	1.448	4.310	7.54	1.750
$1.30P_r$	9°-26′	.9865	.1639	.0269	.6466	.4181	1.406	4.415	8.16	1.850
$1.40P_r$	11°-36′	.9796	.2011	.0404	.6320	.3994	1.368	4.510	8.80	1.950
$1.45P_r$	12°-30′	.9763	.2164	.0468	.6259	.3918	1.353	4.563	9.10	1.995

Table-4.

P	$\sqrt{N}$	$\frac{1}{\sqrt{N}}$	$Q=-A\tau^2R_1^{-\frac{1}{2}}$	$\sin^{-1}(\frac{1}{\sqrt{N}})$	$\sin^{-1}\{\sqrt{N}.\sin(\frac{\pi}{4}-\frac{\alpha}{2})\}$	$\sin^{-1}(\sqrt{N}.\frac{1}{\sqrt{2}})$	$F[\frac{1}{\sqrt{N}},\sin^{-1}\{\sqrt{N}.\sin(\frac{\pi}{4}-\frac{\alpha}{2})\}]$	$E[\frac{1}{\sqrt{N}},\sin^{-1}\{\sqrt{N}.\sin(\frac{\pi}{4}-\frac{\alpha}{2})\}]$	$F\{\frac{1}{\sqrt{N}},\sin^{-1}(\sqrt{N}.\frac{1}{\sqrt{2}})\}$	$E\{\frac{1}{\sqrt{N}},\sin^{-1}(\sqrt{N}.\frac{1}{\sqrt{2}})\}$	$\frac{4Q}{\sqrt{N}}$
$1.05P_r$	1.260	.7936	-1.236	52°-32′	60°-40′	63°-0′	1.191	.950	1.250	.978	-3.925
$1.10P_r$	1.275	.7843	-1.230	51°-40′	60°-17′	64°-22′	1.179	.945	1.276	1.000	-3.860
$1.15P_r$	1.303	.7675	-1.220	50°-8′	61°-6′	67°-7′	1.192	.962	1.335	1.040	-3.745
$1.20P_r$	1.323	.7560	-1.214	49°-7′	61°-12′	73°-12′	1.189	.965	1.479	1.120	-3.670
$1.30P_r$	1.360	.7354	-1.200	47°-20′	61°-34′	74°-6′	1.190	.972	1.486	1.140	-3.530
$1.40P_r$	1.396	.7163	-1.187	45°-45′	61°-55′	81°-14′	1.186	.991	1.649	1.235	-3.400
$1.45P_r$	1.413	.7078	-1.180	45°-3′	62°-10′	87°-36′	1.188	.998	1.803	1.316	-3.340

In deriving Eq. 23, instead of using the value of M_A from Eq. 15 if its closer approximated value be taken from Eq. 31, then we get

$$C_4 = \frac{4Q}{N}\left\{\sqrt{1-N\sin^2\left(\frac{\pi}{4}\frac{\alpha}{2}\right)} - \sqrt{1-\frac{N}{2}}\right\} + \frac{Pr^3}{4EI} + \frac{M_0 r^2}{EI}\sin\alpha. \qquad (23a)$$

Similarly using M_A from Eq. 31 instead of Eq. 15 in the derivation of Eq. 24 we get,

$$C_1 = \frac{2Q}{\sqrt{N}}\left[F\left\{\frac{1}{\sqrt{N}}, \sin^{-1}\left\{\sqrt{N}\sin\left(\frac{\pi}{4}\frac{\alpha}{2}\right)\right\}\right\}\right.$$

$$\left. - 2E\left\{\frac{1}{\sqrt{N}}, \sin^{-1}\left\{\sqrt{N}\sin\left(\frac{\pi}{4}\frac{\alpha}{2}\right)\right\}\right\}\right] + \frac{Pr^3}{4EI}\left(\frac{\pi}{2}-\alpha\right) - \frac{M_0 r^2}{EI}\cos\alpha. \qquad (24a)$$

y_θ at $\theta = 0$ may be expressed from Eq. 12 as

$$y_{\theta=0} = C_4 + \frac{r^2}{EI}\left(M_A - \frac{Pr}{2}\right). \qquad (12a)$$

If we substitute value of $\left(M_A - \frac{Pr}{2}\right)$ from Eq. 6a, Eq. 12a becomes:

$$y_{\theta=0} = C_4 - \frac{r^2}{EI} M_B. \qquad (12b)$$

In Eq. 12b, M_B is to be calculated from Eq. 28 (as in Table 2), while C_4 will be obtained from Eq. 23a.

y_p at $\theta = \frac{\pi}{2}$, may be expressed from Eq. 13 as

$$y_{\theta=\frac{\pi}{2}} = C_1 - \frac{2Q}{\sqrt{N}}\left[F\left\{\frac{1}{\sqrt{N}}, \sin^{-1}\left(\sqrt{N}\,\frac{1}{\sqrt{2}}\right)\right\} - 2E\left\{\frac{1}{\sqrt{N}}, \sin^{-1}\left(\sqrt{N}\,\frac{1}{\sqrt{2}}\right)\right\}\right]. \tag{13a}$$

In Eq. 13a, C_1 is to be evaluated from Eq. 24a. The elliptic integrals are to be evaluted from any standard tables of those integrals (as in Table 4).

a. When load $P = P_0$, $\alpha = 0$, $M_B = M_0$.

Then from Eq. 23a we get

$$C_4 = \frac{P_0 r^3}{4EI},$$

and from Eq. 24a we have

$$C_1 = \frac{2Q}{\sqrt{N}}\left[F\left\{\frac{1}{\sqrt{N}}, \sin^{-1}\left(\sqrt{N}\,\frac{1}{\sqrt{2}}\right)\right\} - 2E\left\{\frac{1}{\sqrt{N}}, \sin^{-1}\left(\sqrt{N}\,\frac{1}{\sqrt{2}}\right)\right\}\right] + \frac{P_0 r^3}{4EI}\,\frac{\pi}{2} - \frac{M_0 r^2}{EI}.$$

Using the value of C_4 and C_1 as obtained above we get from Eq. 12b

$$y_{\theta=0} = \frac{P_0 r^3}{4EI} - \frac{M_0 r^2}{EI}.$$

Substituting value of M_0 from Eq. 33a we get

$$y_{\theta=0} = \frac{P_0 r^3}{4EI} - \frac{P_0 r^3}{EI}\frac{1}{\pi}$$

or

$$y_{\theta=0} = -.0683\,\frac{P_0 r^3}{EI}\,. \qquad (34)$$

From Eq. 13a,

$$y_{\theta=\frac{\pi}{2}} = \frac{2Q}{\sqrt{N}}\left[F\left\{\frac{1}{\sqrt{N}}, \sin^{-1}\left(\sqrt{N}\,\frac{1}{\sqrt{2}}\right)\right\} - 2E\left\{\frac{1}{\sqrt{N}}, \sin^{-1}\left(\sqrt{N}\,\frac{1}{\sqrt{2}}\right)\right\}\right]$$

$$+ \frac{P_0 r^3}{4EI}\,\frac{\pi}{2} - \frac{M_0 r^2}{EI} - \frac{2Q}{\sqrt{N}}\left[F\left\{\frac{1}{\sqrt{N}}, \sin^{-1}\left(\sqrt{N}\,\frac{1}{\sqrt{2}}\right)\right\}\right.$$

$$\left. - 2E\left\{\frac{1}{\sqrt{N}}, \sin^{-1}\left(\sqrt{N}\,\frac{1}{\sqrt{2}}\right)\right\}\right],$$

or

$$y_{\theta=\frac{\pi}{2}} = \frac{P_0 r^3}{EI}\left(\frac{\pi}{8} - \frac{1}{\pi}\right),$$

or

$$y_{\theta=\frac{\pi}{2}} = .0744\,\frac{P_0 r^3}{EI}\,. \qquad (35)$$

Note: At $P = P_0$ the value for y obtained from Eqs. 34 and 35 is essentially the same as that which may be obtained from Eqs. 25 and 26. This similarity in result is expected as at $P = P_0$ the ring, though on the verge of going into plastic range of stress, still obeys Hooke's Law. Thus at $P = P_0$, both the theory of plastic deformation and the elastic

deformation theory are equally applicable to the ring. The negative sign in Eq. 34 indicates the deflection is away from the center of the ring (deflection towards the center was chosen as positive).

b. When $P = 1.05\ P_0$, using Eq. 23a and taking numerical values for different factors from Tables 3 and 4 we get

$$C_4 = -3.115\left\{\sqrt{1-1.588\times.4787} - \sqrt{1-.794}\right\} + 105\times.0198 + 2.52\times.0425,$$

or

$$C_4 = 2.11.$$

Now using Eq. 24a and Tables 3 and 4 we get

$$C_1 = -1.963\left\{1.191-2\times.950\right\} + 105\times.0198\times1.528 - 2.52\times.9991$$

or

$$C_1 = 2.055.$$

Then using Eq. 12b we get

$$y_{\theta=0} = 2.11 - .00428 \times 631$$

or

$$y_{\theta=0} = -.59 \text{ in.}$$

The negative sign indicates a deflection away from the center. Now using Eq. 13a we have

$$y_{\theta=\frac{\pi}{2}} = 2.055 + 1.963 \left\{1.250 - 1.956\right\}$$

or

$$y_{\theta=\frac{\pi}{2}} = .67 \text{ in.}$$

Similarly for all other loads, C_4, C_1, $y_{\theta=0}$ and $y_{\theta=\frac{\pi}{2}}$ are calculated. The results are given in Table 5.

Table 6 shows the comparison between calculated data and the observed data.

B. Corrugated pipe of 36 in. nominal diamter ; .1406 in. plate thickness; corrugations having 2 2/3 in. pitch and 1/2 in. depth.

The average radius of the ring, $r = 18.5$ in.

The elastic limit load from Fig. 11b, $P_0 = 150$ lbs.

By Eq. 33a we have, $M_0 = 883$ lb. in. From Fig. 11b the vertical deflection of the ring Δ_y, by elastic deformation theory is 1.25 in.

Using Eq. 26 we get

$$.0744 \frac{r}{EI} r^2 P_0 = 1.25.$$

Then

$$\frac{r}{EI} = .000329, \quad \frac{r^3}{4EI} = .0282$$

$$\frac{r^2}{EI} = .00608, \quad \frac{M_0 r^2}{EI} = Ar^2 = 5.38.$$

Table 5

P	C_4	C_1	$y_{\theta=0}$ in.	$y_{\theta=\frac{\pi}{2}}$ in.
$1.05P_0$	2.110	2.055	-.59	.67
$1.10P_0$	2.173	2.120	-.65	.72
$1.15P_0$	2.260	2.210	-.70	.81
$1.20P_0$	2.332	2.290	-.76	.89
$1.30P_0$	2.466	2.46	-.89	1.06
$1.40P_0$	2.520	2.700	-1.12	1.31
$1.45P_0$	2.441	2.790	-1.32	1.41

Table 6

Load in in lbs.	Calculated data: change in vert. rad. $y_{\theta=\frac{\pi}{2}}$ in in.		Calculated data: change in hor. rad. $y_{\theta=0}$ in in.		observed data		
	plastic deform. theory	elastic deform. theory*	plastic deform. theory	elastic deform. theory**	Load P in lbs.	$\Delta_y = y_{\theta=\frac{\pi}{2}}$	$\Delta_x = y_{\theta=0}$
0	0	0	0	0	0	0	0
19.05	.113	.112	.104	.103	19.05	.11	.10
38.5	.230	.227	.213	.208	38.5	.24	.21
57.0	.346	.336	.318	.308	57.0	.33	.30
75.5	.461	.445	.425	.407	75.5	.45	.41
90.3	.554	.533	.510	.487	90.3	.55	.49
$100=P_0$	.619	.590	.567	.540	–	–	–
$105=1.05P_0$	.67	.620	.59	.567	104.3	.67	.60
$110=1.10P_0$	.72	.649	.65	.594	–	–	–
$115=1.15P_0$	.81	.678	.70	.621	115.3	.78	.67
$120=1.20P_0$	.89	.708	.76	.648	–	–	–
$130=1.30P_0$	1.06	.766	.89	.702	130.7	1.03	.90
$140=1.40P_0$	1.31	.825	1.12	.756	139	1.28	1.03
$145=1.45P_0$	1.41	.855	1.32	.783	144.1	1.53	1.23
–	–	–	–	–	146.5	1.78	1.43

* Assuming Eq. 26 holds all through.

** Assuming Eq. 25 holds all through.

Table 7

P	a	b	a/b	k*	M_A**	M_B***	a
0	18.5	18.5	1	.1820	0	0	
24.54	18.69	18.30	1.020	.1830	83.7	145	
51.88	18.90	18.07	1.045	.1840	180.2	310	
77.83	19.10	17.85	1.070	.1850	275	468	
102.8	19.28	17.64	1.092	.1860	369	622	
123.7	19.45	17.47	1.115	.1867	449	754	
141.7	19.58	17.32	1.130	.1874	520	867	
$150=P_o$	19.65	17.25	1.140	.1879	554	920	
$165=1.1P_o$	19.77	17.12	1.155	.1885	614	$1015=1.15M_o$	$5°-0'$
$180=1.2P_o$	19.88	17.00	1.170	.1892	676	$1112=1.26M_o$	$7°-56'$
$195=1.3P_o$	20.00	16.87	1.185	.1899	740	$1200=1.36M_o$	$10°-10'$
$210=1.4P_o$	20.11	16.75	1.202	.1906	805	$1307=1.48M_o$	$12°-36'$

* From Table 1

** By Eq. 27

*** By Eq. 28

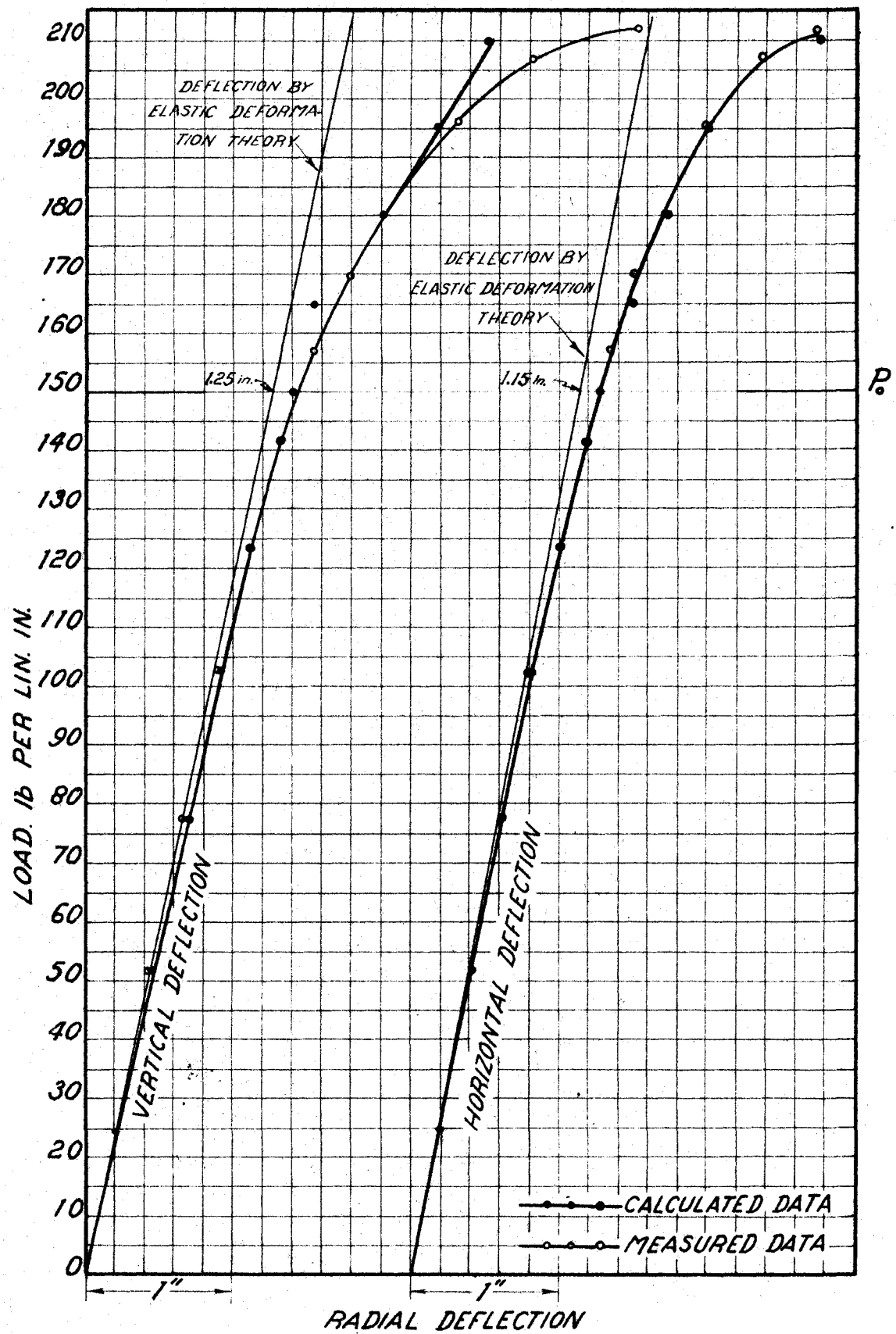
DEFLECTION BY ELASTIC DEFORMATION THEORY
DEFLECTION BY ELASTIC DEFORMATION THEORY
1.25 in.
1.15 in.
P.
LOAD. lb PER LIN. IN.
VERTICAL DEFLECTION
HORIZONTAL DEFLECTION
CALCULATED DATA
MEASURED DATA
1"
1"
RADIAL DEFLECTION

Fig.- 11B.

Table - 8.

P	α	$\cos\alpha$	$\sin\alpha$	$\sin^2\alpha$	$\sin(\frac{\pi}{4}-\frac{\alpha}{2})$	$\sin^2(\frac{\pi}{4}-\frac{\alpha}{2})$	$(\frac{\pi}{2}-\alpha)$	$\frac{P_r}{P_1}=1+\frac{1}{M_0^2}(1-\sin\alpha)$	$R_2=\frac{2P_r}{M_0}$	$N=\frac{R_2}{R_1}$
$1.1P_0$	5°-0′	.9962	.0872	.0076	.6756	.4564	1.484	4.155	6.91	1.662
$1.2P_0$	7°-56′	.9904	.1380	.0190	.6565	.4310	1.432	4.250	7.54	1.775
$1.3P_0$	10°-10′	.9843	.1765	.0312	.6417	.4118	1.393	4.360	8.16	1.873
$1.4P_0$	12°-36′	.9759	.2181	.0476	.6252	.3909	1.351	4.440	8.80	1.986

Table - 9.

P	$\sqrt{N}$	$\frac{1}{\sqrt{N}}$	$Q=-Ar^2R_1^{-\frac{1}{2}}$	$\sin^{-1}(\frac{1}{\sqrt{N}})$	$\sin^{-1}\sqrt{\frac{1}{N}}$, $\sin(\frac{\pi}{4}-\frac{\alpha}{2})$	$\sin^{-1}(\sqrt{N}\cdot\frac{1}{\sqrt{2}})$	$F[\frac{1}{\sqrt{N}}, \sin^{-1}\sqrt{\frac{1}{N}}\cdot\sin(\frac{\pi}{4}-\frac{\alpha}{2})]$	$E[\frac{1}{\sqrt{N}}, \sin^{-1}\sqrt{\frac{1}{N}}\cdot\sin(\frac{\pi}{4}-\frac{\alpha}{2})]$	$F[\frac{1}{\sqrt{N}}, \sin^{-1}(\sqrt{N}\cdot\frac{1}{\sqrt{2}})]$	$E[\frac{1}{\sqrt{N}}, \sin^{-1}(\sqrt{N}\cdot\frac{1}{\sqrt{2}})]$	$\frac{4Q}{\sqrt{N}}$
$1.1P_0$	1.289	.7758	-2.619	50°-53′	60°-33′	65°-43′	1.181	.955	1.307	1.018	-8.127
$1.2P_0$	1.332	.7508	-2.590	48°-40′	61°-0′	70°-22′	1.181	.968	1.407	1.084	-7.778
$1.3P_0$	1.369	.7305	-2.556	46°-56′	61°-28′	75°-28′	1.182	.980	1.518	1.157	-7.469
$1.4P_0$	1.410	.7097	-2.545	45°-13′	61°-45′	85°-4′	1.181	.990	1.737	1.286	-7.225

Table 10

P	C_4	C_1	$y_{\theta=0}$ in.	$y_{\theta=\frac{\pi}{2}}$ in.
$1.1P_0$	4.61	4.50	-1.52	1.54
$1.2P_0$	4.98	4.94	-1.74	2.00
$1.3P_0$	5.25	5.32	-2.02	2.36
$1.4P_0$	5.15	5.70	-2.78	2.7

Table 11

Calculated data					Observed data		
Load P in lbs.	change in vert. rad. $y_{\theta=\frac{\pi}{2}}$ in in.		change in hor. rad. $y_{\theta=0}$ in in.		Load P in lbs.	$\Delta_y = y_{\theta=\frac{\pi}{2}}$	$\Delta_x = y_{\theta=0}$
	plastic deform. theory	elastic deform. theory*	plastic deform. theory	elastic deform. theory**			
0	0	0	0	0	0	0	0
24.54	.206	.204	.190	.188	24.54	.19	.19
51.88	.448	.432	.409	.398	51.88	.41	.41
77.83	.682	.649	.625	.597	77.83	.63	.63
102.8	.914	.856	.838	.782	102.8	.85	.75
123.7	1.119	1.025	1.020	.944	123.7	1.06	.97
141.7	1.295	1.175	1.186	1.08	141.7	1.31	1.16
$150=P_0$	1.385	1.25	1.263	1.15	157.5	1.53	1.34
$165=1.1P_0$	1.54	1.375	1.52	1.265	170.0	1.78	1.50
$180=1.2P_0$	2.00	1.500	1.74	1.38	180.2	2.03	1.69
$195=1.3P_0$	2.36	1.625	2.02	1.495	196.4	2.53	2.00
$210=1.4P_0$	2.7	1.750	2.78	1.610	207.5	3.03	2.38
					212.1	3.72	2.75

* Assuming Eq. 26 holds all through.

** Assuming Eq. 25 holds all through.

IV. DISCUSSION OF THE COMPARISONS

For comparison of the theoretical solutions with results of tests on corrugated pipe the corrugated pipe has been assumed to be a plane circular pipe with an equivalent moment of inertia of the section. The assumption is necessary, as this theory has been developed primarily for a circular ring of rectangular section whose deflection characteristics are the same as that of a plane circular pipe. The equivalent moment of inertia of the assumed plane circular pipe has been obtained from the test data on the corrugated pipe.

From Fig. 11a and Fig. 11b it may be observed that the theoretical solutions check closely with the test data, particularly for the horizontal deflection Δ_x, (see Fig. 8) of the ring, the portion of the ring which does not go into plastic range of stress under the applied load. For the vertical deflection of the ring the theoretical solution also compares very closely with the test data except for very high loads where the theoretical solution gives a smaller deflection value than that obtained from test results. In comparison A, theoretical solution for vertical deflection of the ring compares the test data favorably up to a load of $1.4\ P_0$, whereas in comparison B, it compares with the test data favorably up to a load of $1.3\ P_0$. The difference in the range

of comparison is very possibly due to the fact that the modifications introduced in the equations of moments (Sec. H, Chapter II) in the ring due to the change of its geometry under the load, does not conform closely any more to the actual conditions of the ring under those higher loads; more than 1.4 P_0 in comparison A and 1.3 P_0 in comparison B. The load on the ring up to which the theoretical solution remains comparable with the test data will depend on the percentage deflection at P_0 based on its radius. A higher percentage deflection at P_0 will lower the range in which the theoretical solution and the test data is expected to give a close comparison.

V. POSSIBILITIES OF THE EXTENSION OF THIS THEORY TO FLEXIBLE PIPE CULVERTS UNDER FIELD-LOAD CONDITIONS

As the development of the theory is quite general it seems possible to extend this theory to find the deflection of flexible pipe culverts under field load conditions. It may be recalled that in developing and solving the differential equations we had to consider the moment equation of the ring under load. In order to make the solution general, that is to make the solution applicable to the ring for all loads beyond P_0, we need to assume a constant moment equation for the ring under load. The constants of integrations can be evaluated in the same manner as has been done in this analysis. However, as the assumption of constant moment equation does not hold in reality, due to the successive change in geometry of the ring, modifications must be made in the moment equation of the ring (as has been done in this analysis), later, to calculate approximate values for the deformation of the ring under field load conditions.

The corresponding differential equations for the solution, in case of flexible pipes under field load conditions, are bound to be more involved mathematically, but a preliminary survey showed that even their solution can be carried out with the help of elliptic functions by making proper modifications in the field load conditions.

VI. CONCLUSIONS

A study of the theoretical solution and its comparison with the test data obtained on corrugated pipe justify the following conclusions.

1) The deflection formula developed is satisfactory for determination of the deflection of flexible circular rings acting under two equal and opposite concentrated load when stressed beyond the elastic limit.

2) The theory can be applied to determine deflections of a corrugated pipe under the same loading conditions by assuming it to be a plane circular pipe with an equivalent moment of inertia.

3) The change in geometry of the ring under load affects its moment equations sufficiently to need modifications in actual calculations of deflections.

4) The theory enables one to calculate the radial deflection at any point on the circumference of the ring.

5) The theory developed in this analysis is very general and there are possibilities of its application to flexible pipe culverts under field-load conditions, stressed beyond the elastic limit, by introducing some modifications in the loading condition.

VII. LIST OF REFERENCES

1. Biezeno, C. B. and Koch, J. J. The generalized buckling problem of the circular ring. Nederl. Akad. Wrtensch. Proc. 48:447-468. 1945.

2. Bleich, H. Stahlhochbauten. 1:396-411. Berlin, Julius Springer. 1932.

3. Burke, W. F. Working charts for the stress analysis of elliptic rings. U. S. Nat. Adv. Comm. Aeronaut. Tech. Notes. n. 444. Washington. 1933.

4. Daniels, W. T. Deflection of rigid frames stressed beyond the yield point. Unpublished Ph. D. thesis. Iowa State College. 1941.

5. Gleyzal, A. General stress-strain law of elasticity and plasticity. J. Appl. Mech. 13:A-261-A-264. 1946.

6. Ilyushin, A. A. The theory of plasticity in case of simple loading accompanied by strain hardening. Tech. Memos. U. S. Nat. Adv. Comm. Aeronaut. n. 1207:7. 1949.

7. Ilyushin, A. A. On the theory of plasticity in case of simple loading of plastic bodies with strain hardening. Appl. Math. Mech. (Akad. Nauk. S.S.S.R. Prikl. Mat. Mech.) n. 11:293-296. 1947.

8. Ilyushin, A. A. Relation between the theory of Saint Venant-Levy-Mises and the theory of small elastic-plastic deformations, in plastic deformation (English trans.) by Kachanow, L. N. and others. p. 97-116. Mapleton House, publishers. New York. 1948.

9. Iowa Culvert and Pipe Company. Handbook of Culvert and Drainage Practice. 2nd ed. p. 64. Des Moines, Iowa. 1937.

10. Kachanov, L. M. On the stress-strain relations in the theory of plasticity. C. R. (Doklady) Acad. Sci. URSS. N. S. 54:309-310. 1946.

11. Meyer, E. Von Die Berechnung der Durchbiegung von Staben, deren Material dem Hookeschen Getsetze nicht folgt. Zeitschrift des Vereines deutscher Ingenieure. 58:167-173. 1908.

12. Nadai, A. Plasticity; a mechanics of plastic state of matter. New York. McGraw-Hill. 1931.

13. Pizzetti, Giulio. I solidi a grande curvatura in campo elasto-plastico. Atti-Acca. Sci. Torino. Cl-Sci-Fis. Mat. Nat. 78:31-48. 1943.

14. Prager, William. The stress-strain laws of the mathematical theory of plasticity. A survey of recent progress. J. Appl. Mech. n. 15:226-233. 1948.

15. Scott, E. O. Deformation of beams involving ductile behavior. Unpublished Ph. D. thesis. University of Michigan. 1939.

16. Shafer, G. E. Discussion of flexible pipe culverts. Proc. Highway Research Board (1937) 17:237-239. Highway Research Board, Washington, D. C. 1938.

17. Spangler, M. G. The structural design of flexible pipe culverts. Iowa Eng. Exp. Sta. Bul. 153. 1941.

18. Taylor, G. I. The formation and enlargement of a circular hole in a thin plastic sheet. Quart. Jour. of Mech. and Appl. Math. 1(part 1):103-124. 1948.

19. Van Den Broek, J. A. Limit design. Proc. Am. Soc. of Civ. Eng. 66, n. 8 (part 2):638-661. 1940.

20. Van Den Broek, J. A. Theory of limit design. New York. John Wiley and Sons, Inc. 1948.

21. Winter, George. Discussion of limit design. Proc. Am. Soc. of Civ. Eng. 66, n. 8 (part 2):673-679. 1940.

VIII. ACKNOWLEDGEMENTS

The writer wishes to express his gratitude to Mr. M. G. Spangler, Professor of Civil Engineering; to Dr. Glenn Murphy, Professor of Theoretical and Applied Mechanics; to Dr. B. R. Seth, Visiting Professor of Applied Mathematics; to Dr. R. E. Gaskell, Professor of Mathematics, for their very useful suggestions and criticisms which helped this investigation to its successful completion.

IX. APPENDIX I: DEFLECTION OF A FLEXIBLE CIRCULAR RING DUE TO ITS OWN WEIGHT, SUPPORTED AT THE BASE

The system of forces acting on the ring is shown in Fig. 12a. As the loading system is symmetrical to YY axis, an investigation on a symmetrical half of the ring will reveal its complete deflection characteristics. Fig. 12b shows the free body diagram of one half of the ring.

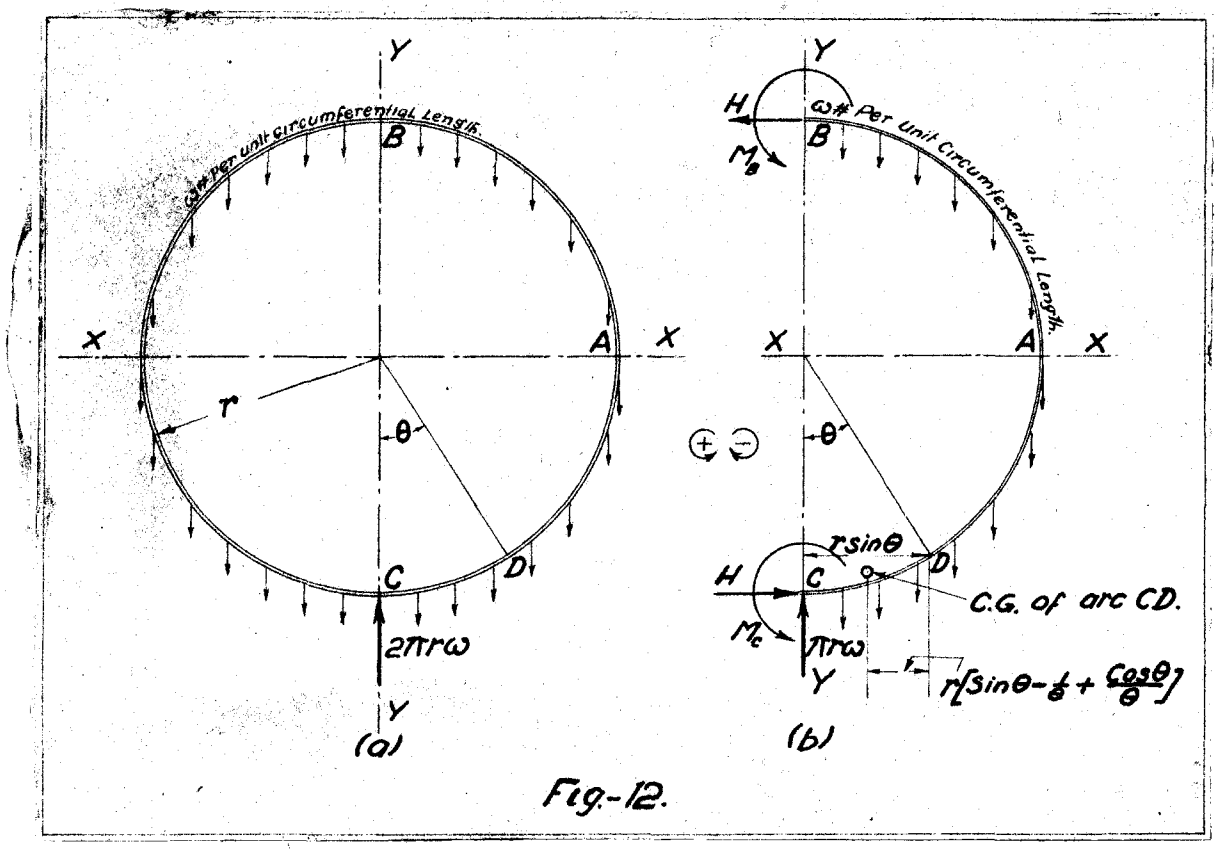

Fig.-12.

From Fig. 12b the general expression for moment at any point D can be written as

$$M = M_c + Hr(1-\cos\theta) - \pi rwr\sin\theta + wr\theta r(\sin\theta - \frac{1}{\theta} + \frac{\cos\theta}{\theta})$$

or

$$M = M_c + Hr(1-\cos\theta) - \pi r^2 w\sin\theta + r^2 w(\theta\sin\theta - 1 + \cos\theta). \qquad (36)$$

Due to the symmetry of the loading system about YY axis we know that tangents to the ring center line remain horizontal at B and C, and therefore the summation of angle changes between C and B equal to $\int_C^B \frac{Mds}{EI}$ must equal zero. The differential length of ring ds = rdθ and the limits C and B represent limits θ = 0 and θ = π respectively. Then we know $\int_0^\pi \frac{r}{EI} Md\theta$, equals zero. Since $\frac{r}{EI}$ is constant in this case we have

$$\int_0^\pi Md\theta = 0. \qquad (37)$$

In Eq. 37 putting the value of M from Eq. 36, we get

$$\int_0^\pi \left[M_c + Hr(1-\cos\theta) - \pi r^2 w\sin\theta + r^2 w(\theta\sin\theta - 1 + \cos\theta) \right] d\theta = 0. \qquad (37a)$$

Evaluating Eq. 37a we get

$$M_c = 2r^2 w - Hr. \qquad (38)$$

Due to the symmetry of the loading system about YY axis we know that the point B does not have any horizontal movement with respect to the tangent to the ring center at C and therefore, the summation of horizontal movement between C and B equal to $\int_C^B \frac{Myds}{EI}$ must equal zero. The differential length of ring $ds = rd\theta$, $y = r(1-\cos\theta)$. Limits C and B represent limits $\theta = 0$, and $\theta = \pi$, respectively. Then we know $\int_0^\pi \frac{r^2}{EI} M(1-\cos\theta)d\theta$ equals zero. Since $\frac{r^2}{EI}$ is constant in this case we have

$$\int_0^\pi M(1-\cos\theta)d\theta = 0$$

or

$$\int_0^\pi Md\theta - \int_0^\pi M\cos\theta\, d\theta = 0.$$

Since $\int_0^\pi Md\theta$ equals zero by Eq. 37. Then we have

$$\int_0^\pi M\cos\theta\, d\theta = 0. \qquad (39)$$

In Eq. 39 putting the value of M from Eq. 36 and the value of M_c from Eq. 38, we get

$$\int_0^\pi \left[r^2w(\theta\sin\theta+1+\cos\theta) - Hr\cos\theta - \pi r^2 w\sin\theta\right]\cos\theta\, d\theta = 0. \qquad (39a)$$

Evaluating Eq. 39a we get

$$H = \frac{\pi w}{2}. \qquad (40)$$

Substituting this value of H in Eq. 38 we have,

$$M_c = 1.5\, r^2 w. \tag{38a}$$

Using values of H and M_c from Eqs. 40 and 38a in Eq. 36 we can write

$$M = r^2 w(1+\theta\sin\theta-\pi\sin\theta+\tfrac{1}{2}\cos\theta). \tag{36a}$$

The vertical displacement of the point B from the tangent drawn to the deflection curve at C which is $2\Delta_y$, can be expressed as

$2\Delta_y = \int_C^B \frac{Mxds}{EI}$, where $x = r\sin\theta$, $ds = rd\theta$, C and B represent limits $\theta = 0$, and $\theta = \frac{\pi}{2}$. Substituting these values in the integral, we have

$$2\Delta_y = \int_0^{\pi} \frac{r^2}{EI} M\sin\theta\, d\theta. \tag{41}$$

In Eq. 41 putting the value of M from Eq. 36a, we have

$$2\Delta_y = \frac{r^2}{EI}\int_0^{\pi} r^2 w(1+\theta\sin\theta-\pi\sin\theta+\tfrac{1}{2}\cos\theta)\sin\theta d\theta. \tag{41a}$$

Evaluating Eq. 41a we get

$$2\Delta_y = -.4674\, \frac{r^4 w}{EI}. \tag{42}$$

The negative sign in Eq. 42 means that the deflection takes place in the negative y direction.

The horizontal displacement of the point C from the tangent drawn to the deflection curve at A which is Δ_x, can be expressed as $\Delta_x = \int_A^C \frac{Myds}{EI}$, where A and C represent limits $\theta = \frac{\pi}{2}$ and $\theta = 0$, respectively. Putting $y = r(1-\cos\theta)$ and $ds = rd\theta$ as before, we get

$$\Delta_x = \int_{\frac{\pi}{2}}^{0} \frac{r^2}{EI} M(1-\cos\theta)d\theta. \qquad (43)$$

In Eq. 43 putting the value of M from Eq. 36a, we have

$$\Delta_x = \frac{r^2}{EI} \int_{\frac{\pi}{2}}^{0} r^2 w(1+\theta\sin\theta-r\sin\theta+\tfrac{1}{2}\cos\theta)(1-\cos\theta)d\theta. \qquad (43a)$$

Evaluating Eq. 43a we get

$$\Delta_x = .2854 \frac{r^4 w}{EI}.$$

Then the total change in the horizontal diameter will be

$$2\Delta_x = .5708 \frac{r^4 w}{EI}. \qquad (44)$$

A. Deflection of a Flexible Corrugated Pipe of Structural Steel due to its Own Weight, Supported at the Base.

The ring analysis made in Appendix I will be valid in case of a flexible corrugated pipe if the effect of axial stress

on the pipe due to the load be neglected. In reality this effect will be small enough to be negligible.

In Eqs. 42 and 44, in case of a corrugated pipe r should be considered to be the mean radius of the pipe. w is the weight per inch length of the corrugated pipe per unit circumferential measure. I is the moment of inertia of the pipe section per inch length of the pipe. E is the modulus of elasticity of the pipe material.

G. E. Shafer (16) of the Armco Drainage Products Association, has developed a simple straight line formula for the moment of inertia per inch length of the cross section of a flexible corrugated pipe with standard corrugations having 2 2/3 in. pitch and 1/2 in. depth. Shafer's formula is

$$I = \frac{t}{30}, \qquad (45)$$

where t = thickness of the metal in inches.

In standard corrugations, a sheet of metal measuring 27.5 inches before corrugation measures 25.5 inches after corrugation (9). Then the length of the metal sheet per inch length of the corrugated sheet will be $\frac{27.5}{25.5}$ inches = 1.078 inches. Then the volume of metal per inch length of the corrugated pipe per inch of circumferential measure (see Fig. 13) becomes vol. = 1(1.078)t cubic inches.

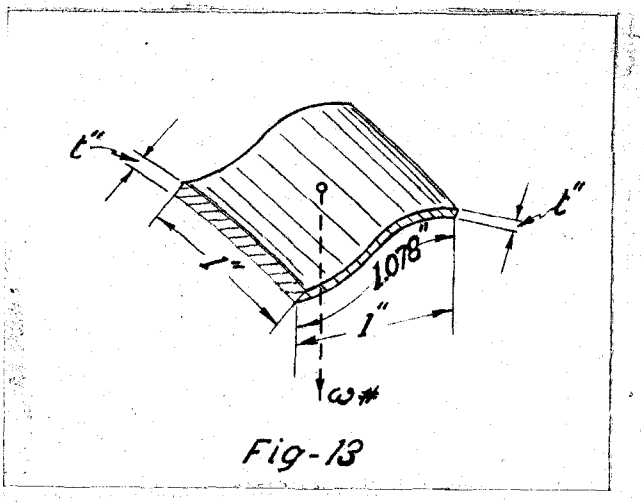

Fig-13

For structural steel we know:

$$\text{sp. weight} = .283 \text{ lb./cu. in.}$$
$$E = 30 \times 10^6 \text{ P.s.i.}$$

Then w, the weight per inch length of the corrugated pipe per inch of circumferential measure can be written as

$$w = .283(1.078)t$$

or

$$w = .3055t. \tag{46}$$

In Eq. 42 using value of I and w from Eqs. 45 and 46 and $E = 30 \times 10^6$, we can write the total change in vertical diameter in magnitude as

$$2\Delta_y = .1428 \times 10^{-6} r^4. \tag{47}$$

Similarly in Eq. 44 putting values of I, w and E we get

$$2\Delta_x = .1744 \times 10^{-6} r^4. \qquad (48)$$

Table 12 shows the changes in the vertical and the horizontal diameter of corrugated flexible pipes having different mean radii due to their own weight when supported at the base. From Fig. 14 deflection due to its own weight for any flexible corrugated pipe having mean radius between 10 inches to 100 inches can be determined.

Table 12

r in inches	$2\Delta_y$ in 10^{-6} inches	$2\Delta_x$ in 10^{-6} inches
1	.1428	.1744
5	89.25	109
10	1,428	1,744
15	7,230	8,830
20	22,840	27,900
25	55,800	68,000
30	115,700	141,100
35	214,000	261,500
40	367,500	446,500
45	585,000	716,000
50	892,500	1,090,000
55	1,308,000	1,595,000
60	1,850,000	2,260,000
65	2,550,000	3,110,000
70	3,443,000	4,190,000
75	4,520,000	5,520,000
80	5,850,000	7,150,000
85	7,450,000	9,100,000
90	9,360,000	11,430,000
95	11,630,000	14,200,000
100	14,280,000	17,440,000

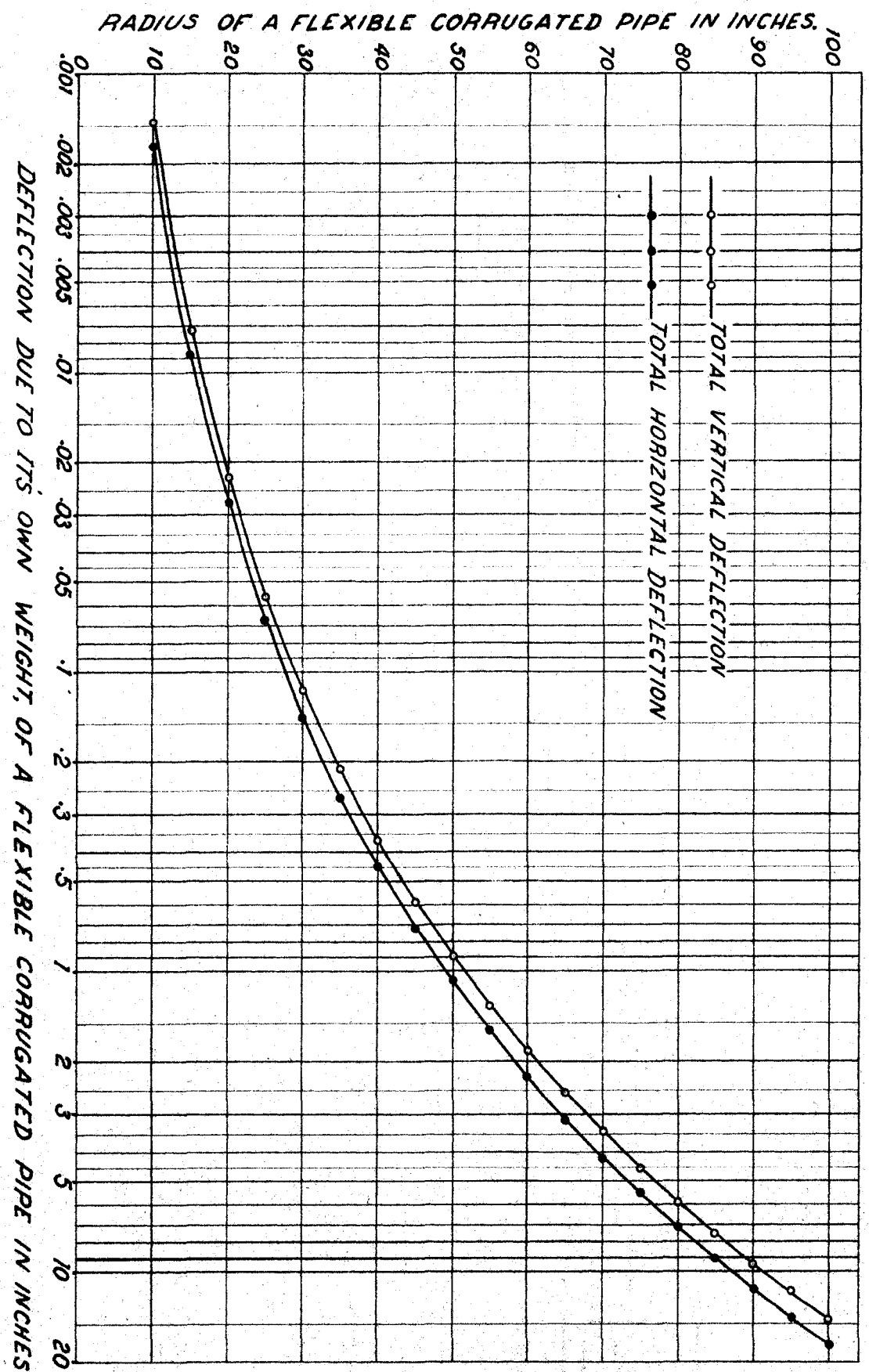
RADIUS OF A FLEXIBLE CORRUGATED PIPE IN INCHES.
0
10
20
30
40
50
60
70
80
90
100
.001
.002
.003
.005
.01
.02
.03
.05
.1
.2
.3
.5
1
2
3
5
10
20
TOTAL VERTICAL DEFLECTION
TOTAL HORIZONTAL DEFLECTION
DEFLECTION DUE TO ITS OWN WEIGHT, OF A FLEXIBLE CORRUGATED PIPE IN INCHES.

Fig-14.

X. APPENDIX II: ELASTIC DEFLECTION OF A FLEXIBLE CORRUGATED PIPE UNDER A MODIFIED FIELD LOAD CONDITION

In the following analysis Spangler's fill-load hypothesis (17 - p. 26) has been modified a little for the simplicity of calculations. In this modification it is assumed that the vertical pressures on the top and bottom of the flexible pipe are uniformly distributed over two horizontal planes at the top and bottom of the conduit having their width equal to the horizontal diameter of the pipe. The horizontal pressure on either side of the flexible pipe is considered to be distributed over two vertical planes, in a triangular manner. The horizontal pressure is a maximum over the horizontal diameter of the conduit and zero at the top and bottom of the conduit. The maximum horizontal pressure is represented by $e\Delta_x$, where e is the modulus of passive pressure of the side fill, and Δ_x is the horizontal radial deflection of the conduit under load.

The distribution of pressures around a flexible pipe under an earth fill, according to this modified field load condition is shown graphically in Fig. 15.

Under such modified loading condition it is possible to express the moments, thrusts, shears, and deflections of a pipe as continuous functions of the properties of the pipe and of the soil of which the side fills are constructed.

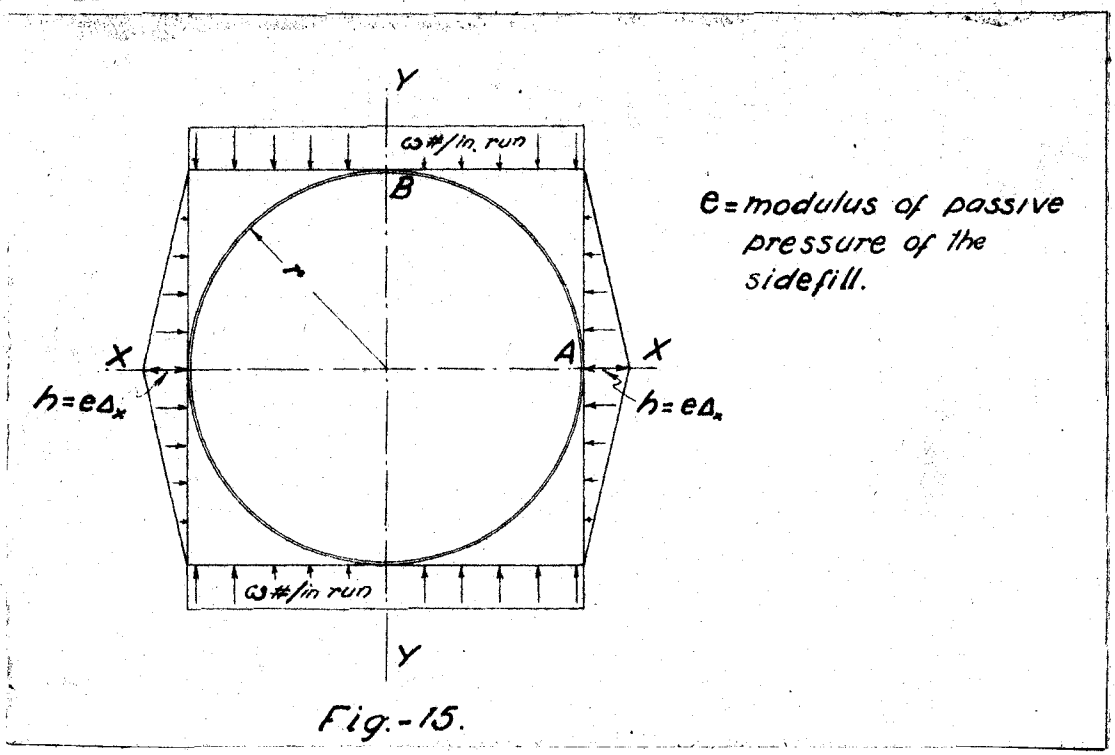

Fig.-15.

As the loading system is symmetrical with respect to both XX and YY axis, an investigation on a quarter of the ring will reveal its complete deflection characteristics. Fig. 16a shows the free body diagram of one quarter of the ring. Fig. 16b shows the position of the C. G. (center of gravity) of a trapezoidal area.

The general expression for moment at any point D(Fig. 16a) in the ring can be written as:

$$M = wrr(1-\cos\theta) + M_A - (h-\frac{h}{2}\sin\theta)r\sin\theta\,\frac{r\sin\theta(3-\sin\theta)}{3(2-\sin\theta)}$$

$$- wr(1-\cos\theta)\,\frac{r(1-\cos\theta)}{2}$$

or

$$M = wr^2(1-\cos\theta) + M_A - \frac{1}{6}hr^2\sin^2\theta(3-\sin\theta) - \frac{1}{2}wr^2(1-\cos\theta)^2. \qquad (49)$$

Due to the symmetry of structure and loading system we

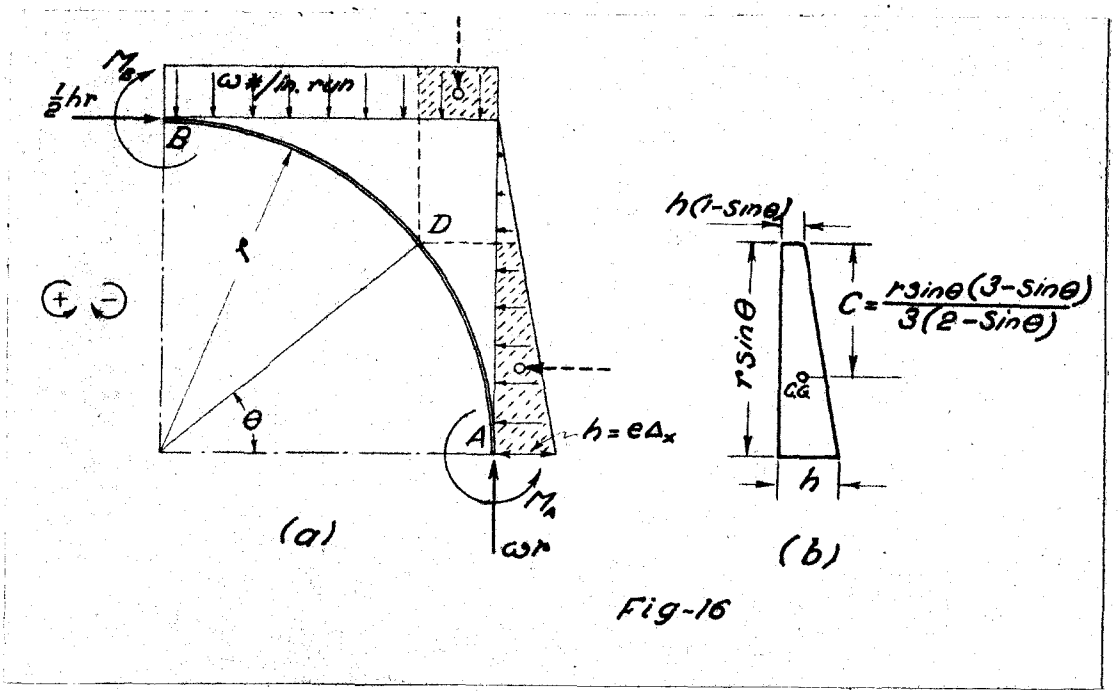

Fig-16

know that tangents to the ring center line remain horizontal at B and vertical at A and therefore the summation of angle changes between A and B, equal to $\int_A^B \frac{Mds}{EI}$ must equal zero. Since EI is constant in this case, we have $\int_A^B Mds = 0$.

The differential length of ring $ds = rd\theta$ and the limits A and B represent limits $\theta = 0$ and $\theta = \frac{\pi}{2}$, respectively.

Then $\int_0^{\frac{\pi}{2}} Mrd\theta = 0$. As r is a constant, we have

$$\int_0^{\frac{\pi}{2}} Md\theta = 0. \qquad (50)$$

In Eq. 50 putting the value of M from Eq. 49, we get

$$\int_0^{\frac{\pi}{2}} \left[wr^2(1-\cos\theta) + M_A - \frac{1}{6}hr^2\sin^2\theta(3-\sin\theta) - \frac{1}{2}wr^2(1-\cos\theta)^2\right] d\theta = 0. \qquad (50a)$$

Evaluating Eq. 50a we can find

$$M_A = hr^2\left(\frac{1}{4} - \frac{2}{9\pi}\right) - \frac{1}{4}wr^2. \qquad (51)$$

Substituting the value of M_A in Eq. 49, we get M as

$$M = \frac{1}{2}wr^2\sin^2\theta + hr^2\left(\frac{1}{4}-\frac{2}{9\pi}\right) - \frac{1}{4}wr^2 - \frac{1}{6}hr^2\sin^2\theta(3-\sin\theta). \qquad (49a)$$

At $\theta = \frac{\pi}{2}$, $M = M_B$. Then

$$M_B = \frac{1}{4}wr^2 - hr^2\left(\frac{1}{12}+\frac{2}{9\pi}\right). \qquad (52)$$

If we consider A and B to be two points on the deflection curve of the loaded ring, the horizontal displacement of B from the tangent drawn to the deflection curve at A, which is Δ_x, can be expressed as:

$$\Delta_x = \int_A^B \frac{Myds}{EI},$$

where $ds = rd\theta$, $y = r\sin\theta$, the limits of integration A and B represent limits $\theta = 0$, and $\theta = \frac{\pi}{2}$, respectively.

Then we have

$$\Delta_x = \frac{r^2}{EI} \int_0^{\frac{\pi}{2}} M \sin\theta d\theta. \qquad (53)$$

Similarly the vertical displacement of A from the tangent drawn to the deflection curve at B, which is Δ_y, can be expressed as

$$\Delta_y = \int_B^A \frac{Mxds}{EI},$$

where $x = r\cos\theta$, and other notations have the same values as in case of Δ_x.

Then we have

$$\Delta_y = \frac{r^2}{EI} \int_{\frac{\pi}{2}}^0 M\cos\theta d\theta. \qquad (54)$$

In Eq. 53 substituting the value of M from Eq. 49a we get

$$\Delta_x = \frac{r^2}{EI} \int_0^{\frac{\pi}{2}} \left[hr^2\left(\frac{1}{4} \frac{2}{9\pi}\right) - \frac{1}{4}wr^2 + \frac{1}{2}wr^2\sin^2\theta \right.$$

$$\left. - \frac{1}{6} hr^2\sin^2\theta(3-\sin\theta) \right] \sin\theta d\theta. \qquad (53a)$$

Evaluating Eq. 53a and substituting value of $h = e\Delta_x$, we get

$$\Delta_x = \frac{wr^4}{6EI + .336r^4 e}. \qquad (55)$$

Similarly substituting value of M in Eq. 54, and evaluating

the integral we get

$$\Delta_y = \frac{wr^4}{6EI+.336r^4e}\left(1+\frac{.0018r^4e}{EI}\right). \qquad (56)$$

Spangler's formula for horizontal deflection[1] of a flexible pipe culvert acting under his fill-load hypothesis[2], when the bedding angle a equals 90°, reduces to

$$\Delta_x = \frac{wr^4}{6EI+.336r^4e}. \qquad (57)$$

Eqs. 55 and 57 give a comparison between the results obtained by this modified field load condition and Spangler's fill-load hypothesis. A comparison with the experimental data[3] shows that Eq. 55 will give closer results to the observed data than those obtained by Eq. 57.

---

[1] Spangler, M. G. The structural design of flexible pipe culverts. Iowa Eng. Exp. Sta. Bul. 153, p. 29. 1941.

[2] Ibid. p. 26.

[3] Ibid. p. 79.